LIMNOLOGY
and
OCEANOGRAPHY

ASLO

Limnol. Oceanogr. 00, 2017, 00–00

doi: 10.1002/lno.10554

Shelf-basin gradients shape ecological phytoplankton niches and community composition in the coastal Arctic Ocean (Beaufort Sea)

M. Ardyna [1,2]* M. Babin,[1] E. Devred,[1] A. Forest,[1] M. Gosselin [3] P. Raimbault,[4] J.-É. Tremblay[1]

[1]Takuvik Joint International Laboratory, Laval University (Canada) - CNRS (France), UMI3376, Département de biologie et Québec-Océan, Université Laval, Québec, Québec, Canada

[2]Sorbonne Universités, UPMC Univ Paris 06, INSU-CNRS, Laboratoire d'Océanographie de Villefranche, Villefranche-sur-mer, France

[3]Institut des sciences de la mer de Rimouski, Université du Québec à Rimouski, Rimouski, Québec, Canada

[4]Aix-Marseille University, Mediterranean Institute of Oceanography (MIO), UMR7294, CNRS/INSU, UMR235, IRD, Marseille, CEDEX 09, France

Abstract

The contiguous Arctic shelf is the green belt of the Arctic Ocean. Phytoplankton dynamics in this environment are driven by extreme physical gradients and by rapid climate change, which influence light and nutrient availability as well as the growth and ecological characteristics of phytoplankton. A large dataset collected across the Canadian Beaufort Shelf during summer 2009 was analyzed to assess how the interplay of physical and biogeochemical conditions dictates phytoplankton niches and trophic regimes. Nonmetric multidimensional scaling and cluster analysis demonstrated marked partitioning of phytoplankton diversity. Elevated phytoplankton biomass ($\sim$ 2.41 μg Chl *a* L^{-1}) was observed in association with the surface mixed layer near the coast, close to the mouth of the Mackenzie River, and at the shelf-break as a result of nutrient-rich Pacific water intrusions. The coastal communities were supported by high levels of nitrogen nutrients and were taxonomically uniform, with diatoms accounting for 95% of total cell numbers. By contrast, adjacent oceanic waters were characterized by low autotrophic biomass near the surface ($\sim$ 0.09 μg Chl *a* L^{-1}) and below the mixed layer ($\sim$ 0.23 μg Chl *a* L^{-1}) due to mainly nutrient limitation. However, the oceanic community was more diverse with a mixed assemblage of diatoms and small mixotrophs/heterotrophs near the surface and a predominance of autotrophic nanoflagellates at depth. We conclude that as climate change intensifies freshening and stratification in the Western Arctic Ocean, coastal hotspots of high autotrophic productivity may play an even greater role in supporting Arctic marine ecosystems while offshore environments become increasingly oligotrophic.

The Arctic Ocean is characterized by a high seasonality (i.e., alternation between the polar night and day, a short growing season and a presence of a sea-ice cover) that imposes contrasted growth conditions to phytoplankton (Harrison and Cota 1991; Grebmeier et al. 1995; Sakshaug 2004) and has direct consequences on their vertical distribution and community composition (Li et al. 2009; Tremblay et al. 2009; Ardyna et al. 2011; Terrado et al. 2012), productivity (Arrigo and Van Dijken 2015; Hill et al. 2017; Blais et al. 2017), and phenology (Kahru et al. 2010; Ji et al. 2012; Ardyna et al. 2014). In a context of rapid environmental changes, a mosaic of limiting growth factors is altered and modifies the Arctic ecological phytoplankton niches and productivity and their interactions with higher trophic levels (Poulin et al. 2011; Lovejoy 2014).

Nutrient supply (i.e., mainly nitrate) sets spatial pan-Arctic differences in trophic status (i.e., oligotrophic vs. eutrophic), whereas light availability modulates the productive period within each regime (Codispoti et al. 2013; Varela et al. 2013; Tremblay et al. 2015). These different productivity regimes are expected to respond differently to current and future Arctic change, depending mostly on the strength of the vertical stratification and on episodically or periodically forcing events (e.g., wind-driven upwelling or topographically-enhanced mixing) (Ardyna et al. 2011; Michel et al. 2015). With the ongoing receding of sea-ice and a longer open-water period, the coastal Arctic regions (or, namely interior shelves) are more susceptible to the upwelling of nutrient-rich water across the shelf-break (Williams and Carmack

*Correspondence: Mathieu.Ardyna@obs-vlfr.fr

2015). Such events trigger sudden and localized increases in productivity throughout the Arctic marine ecosystem (Tremblay et al. 2011), thus creating hotspots for higher trophic levels (Walkusz et al. 2012; Conlan et al. 2013; Citta et al. 2015). However, the shaping effects of coastal nutrient supply on ecological phytoplankton niches and trophic regimes that have a high potential for carbon transfer remain to be assessed at a pan-Arctic scale.

In the oligotrophic western Arctic Ocean (Beaufort Gyre), surface water freshening and nitracline deepening exacerbate nitrogen limitation of phytoplankton communities (McLaughlin and Carmack 2010; Coupel et al. 2015*b*). As a consequence, widespread subsurface phytoplankton layers (namely subsurface chlorophyll maxima [SCMs]) subsist during the post-bloom period at the optimal depth where light availability and upward nutrient flux are sufficient to sustain phytoplankton growth (Ardyna et al. 2013; Brown et al. 2015; Martini et al. 2016). During the deepening of the SCM following the surface nitrate drawdown in spring, a loss of productivity has been observed associated with a transition of phytoplankton communities from new production to regenerated production in the Canadian Arctic (Garneau et al. 2007; Martin et al. 2012). In highly stratified and oligotrophic Arctic regions, the deepening of the SCM has been related to a shift from autotrophic to heterotrophic communities (Monier et al. 2014).

Within this context, a more comprehensive ecological understanding of the impact of nitrogen cycling on vertical phytoplankton distribution and composition is critical. Here, we investigate the ecological processes responsible for shaping ecological phytoplankton niches, productivity, and their trophic regime in an interior shelf, the southeastern Beaufort Sea as part of the 2009 "Mackenzie Light and Carbon" (MALINA) project. These interior shelves comprise approximately 40% of the total Arctic shelf area (2.5×10^6 km^2, Williams and Carmack 2015) and are generally characterized by extreme shelf-basin gradients, which significantly affect light propagation and nutrient dynamics (Carmack et al. 2004; Forest et al. 2011, 2014; Doxaran et al. 2012; Antoine et al. 2013; Tremblay et al. 2014). The major objectives of the current study are: (1) to characterize the phytoplankton community structure associated with SCMs and with the surface layer; and (2) to identify the environmental factors driving the formation, maintenance, and productivity of coastal (< 50 m) and oceanic (≥ 50 m) SCMs. Using the large dataset collected here, we also aim at assessing the role of key physical and biological determinants underlying the patterns of variation in phytoplankton vertical distribution and composition. Such knowledge is fundamental for improving our conceptual understanding of carbon cycling in the coastal Arctic Ocean and thus our ability to predict future changes in this environment.

Methods

Study area and sampling design

The oceanographic sampling was conducted from 02 July 2009 to 25 August 2009 during the MALINA expedition on the CCGS *Amundsen* in the southeastern Beaufort Sea (Fig. 1). The Mackenzie Shelf is a narrow rectangular shelf (120 km width $\times$ 530 km length) bounded by the Alaskan Beaufort Shelf in the west, the Amundsen Gulf in the east, and by the Canada Basin in the north. A total of 141 stations, located both in coastal (< 50 m) and oceanic (≥ 50 m) waters, were visited during the cruise providing detailed information on shelf-basin transitions (Fig. 1, red lines).

At each station, water samples were collected at 6–10 discrete depths (including the depth of the SCM) with a rosette sampler equipped with 12-L Niskin-type bottles (OceanTest Equipment, $n = 24$) in addition to profiles measured using a Sea-Bird 911plus conductivity temperature depth (CTD) probe for salinity and temperature measurements, a transmissometer (Wetlabs C-Star, path 25 cm) for beam attenuation measurement, a nitrate sensor (ISUS V2, Satlantic), and a chlorophyll fluorometer (SeaPoint). Fluorescence and nitrate measurements from the sensor mounted on the CTD were post-calibrated from analytically determined chlorophyll *a* (Chl *a*) and nitrate concentrations (only used here to derive the depth and the steepness of the nitracline) following the procedures from Martin et al. (2010) and Forest et al. (2014). The depth of the euphotic zone (defined as 1% of surface irradiance) was estimated from the photosynthetically active radiation (400–700 nm) profile obtained with a Biospherical QCP-2300 spherical cosine sensor.

To identify phytoplankton niches and productivity regimes in the southeastern Beaufort Sea, we first identified two distinct phytoplankton chlorophyll maxima occurring along the vertical profile: (1) the surface chlorophyll maximum (SUCM) which corresponds to the maximum chlorophyll concentration (> 0.2 $\mu g\ L^{-1}$) within the surface mixed layer; and (2) the SCM that corresponds to the maximum chlorophyll concentration (> 0.2 $\mu g\ L^{-1}$) below the surface mixed layer. We subsequently define four distinct spatial domains where these two phytoplankton vertical features may occur. These four domains (upper surface coastal water [UC], lower subsurface coastal water at the depth of SCM [SC], upper surface oceanic water [UO], and lower subsurface oceanic water at the depth of SCM [SO]; *see* their definitions in Table 1) are based on bottom depth, with the 50 m isobath as the criteria to distinguish coastal and oceanic waters (following the previous delimitation defined in Ardyna et al. 2013); and on the mixed-layer depth as the vertical boundary. Further definitions and descriptions of the two distinct phytoplankton vertical features and of the four spatial domains are summarized in Table 1.

Nutrients, Chl *a*, and particulate organic carbon

Nutrients, Chl *a* concentrations, and particulate organic carbon (POC) were determined at 6–10 discrete depths in the upper 200 m of the water column, including the depth of

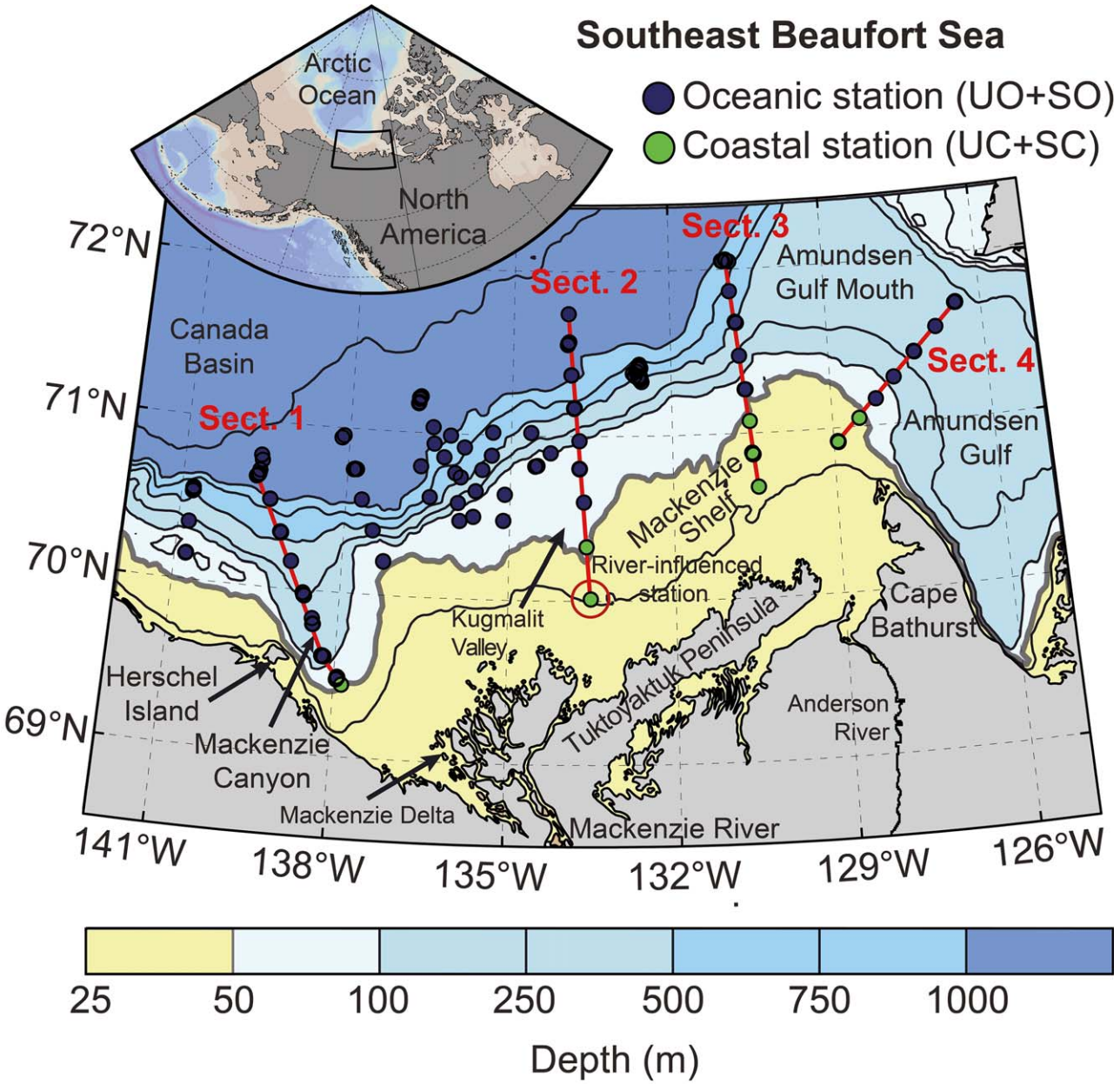

Fig. 1. Location of sampling stations (i.e., coastal (< 50 m; UC, upper surface coastal water; SC, lower subsurface coastal water at the depth of SCM) and oceanic (≥ 50 m; UO, upper surface oceanic water; SO, lower subsurface oceanic water at the depth of SCM) stations) for the MALINA cruise in the southeastern Beaufort Sea, Canadian Arctic. The bathymetry is extracted from the International Bathymetric Chart of the Arctic Ocean (Jakobsson et al. 2012). The red lines indicate the four sections discussed in the present study (referred to sections 1–4 from left to right).

the SCM. Ammonium concentrations were measured on board immediately after sampling using the sensitive method of Holmes et al. (1999) with a detection limit of 5 nmol L^{-1}. Samples for nitrate, nitrite, phosphate, and silicate determination were collected into 20 mL polyethylene flasks and immediately poisoned with mercuric chloride (10 μg mL^{-1}), according to Kirkwood (1992), and stored for subsequent laboratory analysis. Nitrate and nitrite concentrations (lower detection limit = 3 nmol L^{-1}) were obtained using the sensitive method of Raimbault et al. (1990). Nitrate in deep waters (detection limit = 0.05 μmol L^{-1}) and phosphate (detection limit = 0.02 μmol L^{-1}) were measured according to the method of Aminot and Kérouel (2007).

Chl *a* concentrations were determined by high performance liquid chromatography (HPLC), following the method described in Ras et al. (2008). Seawater aliquots ranging from 0.25 L to 2.27 L were filtered through 25 mm Whatman GF/F glass-fiber filters (nominal pore size of

Table 1. Abbreviation, definition, and description of phytoplankton vertical features and the spatial domain they occupy in the Beaufort Sea. See Table 4 for the description of spatial domains in terms of physical and biogeochemical properties.

Abbreviation	Definition	Description
Phytoplankton vertical features		
SUCM	Surface chlorophyll maximum	Chl *a* >0.2 μg L^{-1}; within the surface mixed layer
SCM	Subsurface chlorophyll maximum	Chl *a* >0.2 μg L^{-1}; below the surface mixed layer
Spatial domains		
UC	Upper surface coastal water	Bottom depth <50 m; within the surface mixed layer
SC	Lower subsurface coastal water at the depth of SCM	Bottom depth <50 m; below the surface mixed layer
UO	Upper surface oceanic water	Bottom depth ≥50 m; within the surface mixed layer
SO	Lower subsurface oceanic water at the depth of SCM	Bottom depth ≥50 m; below the surface mixed layer

Note: the depth of the surface mixed layer was defined as the depth where the Brunt-Väisälä frequency was greatest.

0.7 μm), frozen immediately in liquid nitrogen and then stored at −80°C until analysis. Analyses were performed at the Laboratoire d'Océanographie de Villefranche (LOV). Filters were extracted in 3 mL methanol (100%) for 2 h, disrupted by sonication, centrifuged, and filtered (Whatman GF/F). The extracts were injected within 24 h onto a reversed phase C8 Zorbax Eclipse column (dimensions: 3 × 150 mm; 3.5 μm pore size), to estimate Chl *a* concentrations.

Samples for POC were filtered onto 25 mm Whatman GF/F filters pre-combusted at 500°C for 4 h. Between 250 mL and 1200 mL of sample was filtered depending on the quantity of particulate matter in the sample. The filters were then washed with 100 μL of H_2SO_4 (0.5 N) to remove inorganic carbon. The filters were then stored in 25 mL Schott glass bottles for laboratory analysis. Blank filters were prepared for each set of samples by washing the filter with 200 mL of 0.2 μm-filtered seawater. Determination of POC was performed following the wet-oxidation procedure described in Raimbault et al. (1999*a*).

Phytoplankton abundance and taxonomic composition

Samples taken within the surface mixed layer and at the depth of SCM for the identification and enumeration of phytoplankton and other protists > 2 μm were preserved in acidic Lugol's solution (final concentration of 0.4%) (Parsons et al. 1984) and stored in the dark at 4°C until analysis. Cell identification was carried out at the lowest possible taxonomic level using an inverted microscope (Wild Heerbrugg and Zeiss Axiovert 10) following the Utermöhl method using settling columns of 25 mL and 50 mL (Lund et al. 1958). A minimum of 400 cells (accuracy: 10%) and three transects were counted at a magnification of 200X and 400X. The main taxonomic references used to identify the phytoplankton were Tomas (1997) and Bérard-Therriault et al. (1999).

Uptake and regeneration rates

Rates of carbon fixation, nitrate uptake, and ammonium regeneration/uptake were measured at a subset of stations using a dual ^{13}C-^{15}N isotopic technique (Raimbault et al. 1999). Samples were collected within the surface mixed layer and at the depth of the SCM, and subsamples were poured into 600-mL polycarbonate flasks, previously rinsed with 10% HCl, then with ultra-pure Milli-Q water. Labelled sodium bicarbonate ($NaH^{13}CO_3$ 36 g L^{-1} – 99.7 atom % ^{13}C, EURISOTOP) was added to each bottle in order to obtain ≈ 10% final enrichment (0.5 mL/600 mL seawater). Nitrogen ^{15}N-tracer additions, $K^{15}NO_3$ or $^{15}NH_4Cl$ (99 atom % at ^{15}N), were 10% or 20% of the ambient concentration based on measurements made on previous casts. In nutrient impoverished waters, when concentrations were lower than the detection limit, additions of ^{15}N were fixed at 17 ± 3 nmol L^{-1} for ^{15}N-NO_3 and 43 ± 3 nmol L^{-1} for ^{15}N-NH_4. This procedure has already been applied in ultra-oligotrophic waters (South-West Pacific) with no detectable stimulation of primary production (*see* Fig. 10 in Raimbault and Garcia 2008).

Incubations were started immediately following tracer addition, just before dawn in an on-deck incubator. Light levels were adjusted with a combination of blue and neutral density screens to simulate conditions at the depths of collection. The incubator was maintained at sea-surface temperature using pumped seawater. After 24 h, samples were filtered through precombusted (450°C) Whatman GF/F filters using a low vacuum pressure (< 100 mm Hg). The ^{15}N-NH_4 filtrates were collected in Duran Schott glass flasks and poisoned with 1 mL $HgCl_2$ (6 g L^{-1}) in order to prevent bacterial activity during storage. GF/F filtrates from the $^{15}NH_4$ incubations were used to measure the final ^{15}N enrichment in the NH_4 pool and the estimation of the isotope dilution of the tracer due to NH_4 regeneration as outlined by Raimbault et al. (1999*b*). GF/F filtrates from the $^{15}NH_4$ incubations were used to measure the final ^{15}N enrichment in the NH_4 pool as outlined by Raimbault et al. (1999). Ammonium regeneration rates were then estimated from the isotope dilution of the $^{15}NH_4$ tracer according to Laws (1984).

Following filtration, filters were placed into 2 mL glass tubes, dried for 24 h in a 60°C oven and stored dry until laboratory analysis. These filters were used to determine the final $^{15}N/^{13}C$ enrichment ratio in the particulate organic matter and the concentrations of particulate carbon and

particulate nitrogen. The dual isotopic enrichment analysis was performed on an Integra-CN mass spectrometer calibrated using glycine references every batch of 10–15 samples. The accuracy of our analytical system was regularly verified using reference materials from the International Atomic Energy Agency (IAEA, Analytical Quality Control Services) showing correct ^{15}N atom % determination over a large range of nitrogen amount (0.2–10 μmol N). Thus, the low background of the system gave an accurate analysis for samples containing low nitrogen amount (0.1–0.2 μmol), values often observed in surface oligotrophic waters. For ^{15}N-NO_3 and ^{15}N-NH_4 experiments, time 0 enrichment was 0.372% ± 0.007%. We considered the results to be significant when ^{15}N excess enrichments were greater than 0.014% (two times the standard deviation obtained with time zero samples).

Calculation and statistical analyses

The vertical distribution of water masses was defined using salinity data collected by CTD casts according to previous studies (Rudels et al. 2004; Aksenov et al. 2010) and are summarized in Table 2. The depths of the surface mixed layer and of the nitracline were defined as the depth where the Brunt-Väisälä frequency and the vertical gradient in nitrate concentration (dNO_3/dz) were greatest. In addition to the nitracline depth, a second nitracline property was derived from the CTD-nitrate calibrated data: the steepness of the nitracline, which is a proxy for the upward flux of nitrate (Aksnes et al. 2007). The steepness of the nitracline was determined using the following linear interpolation: $(NO_3(2)-NO_3(1))/(z(2)-z(1))$, where (1) and (2) are respectively the uppermost and lowermost depths delimiting the nitracline vertically as visually inspected. Such assessment of the nitracline steepness is particularly relevant when direct measurements of vertical nitrate flux are not available. The steepness of the nitracline is expected to be function of the upward nitrate fluxes and of the strength of the turbulent mixing that sustains them despite any biological consumption.

Based on the CTD-fluorescence profiles, the depth of the SCM was defined as the depth where the in vivo fluorescence reached a maximum (Table 1). In several fluorescence profiles, a second maximum was also observed close to the surface, which is defined as the surface chlorophyll maximum, SUCM. In both cases, a minimum Chl *a* concentration of 0.2 $\mu g\ L^{-1}$ was used to define the presence or absence of a SUCM or SCM. The distinction between SUCM and SCM was based on the surface mixed layer depth as described above. The SUCM is located above or in the vicinity of the surface mixed layer depth, while the SCM would occur below it.

A one-way analysis of variance by ranks (Kruskal–Wallis *H*-test) was performed to test whether the four domains of the Beaufort Sea (*see* Table 1) differed in their environmental and biological variables (Zar 1999). A significant result of the Kruskal–Wallis *H*-test implies that at least one domain differs from all others. We then applied a post hoc test (Chi-square test) to identify which domains differ significantly from others ($p < 0.05$) (Wheater and Cook 2005).

Table 2. Water mass characteristics of the study area as defined in Aksenov et al. (2010) and Rudels et al. (2004).

Acronym	Water mass	Definition
UPML	Upper polar mixed layer	Salinity $<$ 29
LPML	Lower polar mixed layer	29 $\leq$ Salinity $<$ 30.8
PSW	Pacific summer water	30.8 $\leq$ Salinity $<$ 32.1
UHW	Upper halocline water	32.1 $\leq$ Salinity $<$ 33.9
LHW	Lower halocline water	33.9 $\leq$ Salinity $<$ 34.7
AW	Atlantic water	Salinity $\geq$ 34.7

A nonmetric multidimensional scaling (nMDS) ordination of a Bray-Curtis similarity matrix coupled with a group-average cluster analysis was performed on taxonomic data (i.e., samples at both the surface and the depth of SCM) to characterize groups of stations with similar composition (Clarke and Warwick 2001), using the R statistical software (package vegan v2.3-2). The relative abundances of 15 taxonomic groups (centric and pennate diatoms, dinoflagellates, chlorophytes, choanoflagellates, chrysophytes, cryptophytes, dictyophytes, euglenophytes, prasinophytes, prymnesiophytes, raphidophytes, unidentified flagellates, ciliates, and heterotrophic groups) were used to calculate the Bray-Curtis similarity matrix.

An analysis of similarities (one-way ANOSIM) was performed on the Bray-Curtis similarity matrix to identify groups of stations with significantly different taxonomic compositions (Clarke and Warwick 2001). A breakdown of species similarities (SIMPER) was then performed to determine which taxonomic entry combination led to the resulting groups (Clarke 1993).

Results and discussion

The Beaufort Sea ecosystem exhibits distinct phytoplankton vertical profiles according to a given location across the shelf, slope, and basin environments. Physical and biogeochemical gradients across this shelf-basin interface are shown with in situ data collected along four sections visited during MALINA (Fig. 1) and summarized in Fig. 2. Each of these sections shows: (1) the isohalines (shown as black lines), (2) the vertical distribution of the water masses (listed and defined in Table 2), and (3) the depth of the mixed layer, the nitracline, the base of the euphotic zone, and the maximum surface and subsurface fluorescence (i.e., SUCM and SCM). The SUCM is located above or in the vicinity of the surface mixed layer depth, while the SCM would occur below it. It is noteworthy that the base of the euphotic zone is usually well below the surface mixed layer depth (up to several tens of meters) during the typical late summer conditions in the Beaufort Sea (Fig. 2; *see* also Carmack and Macdonald 2002

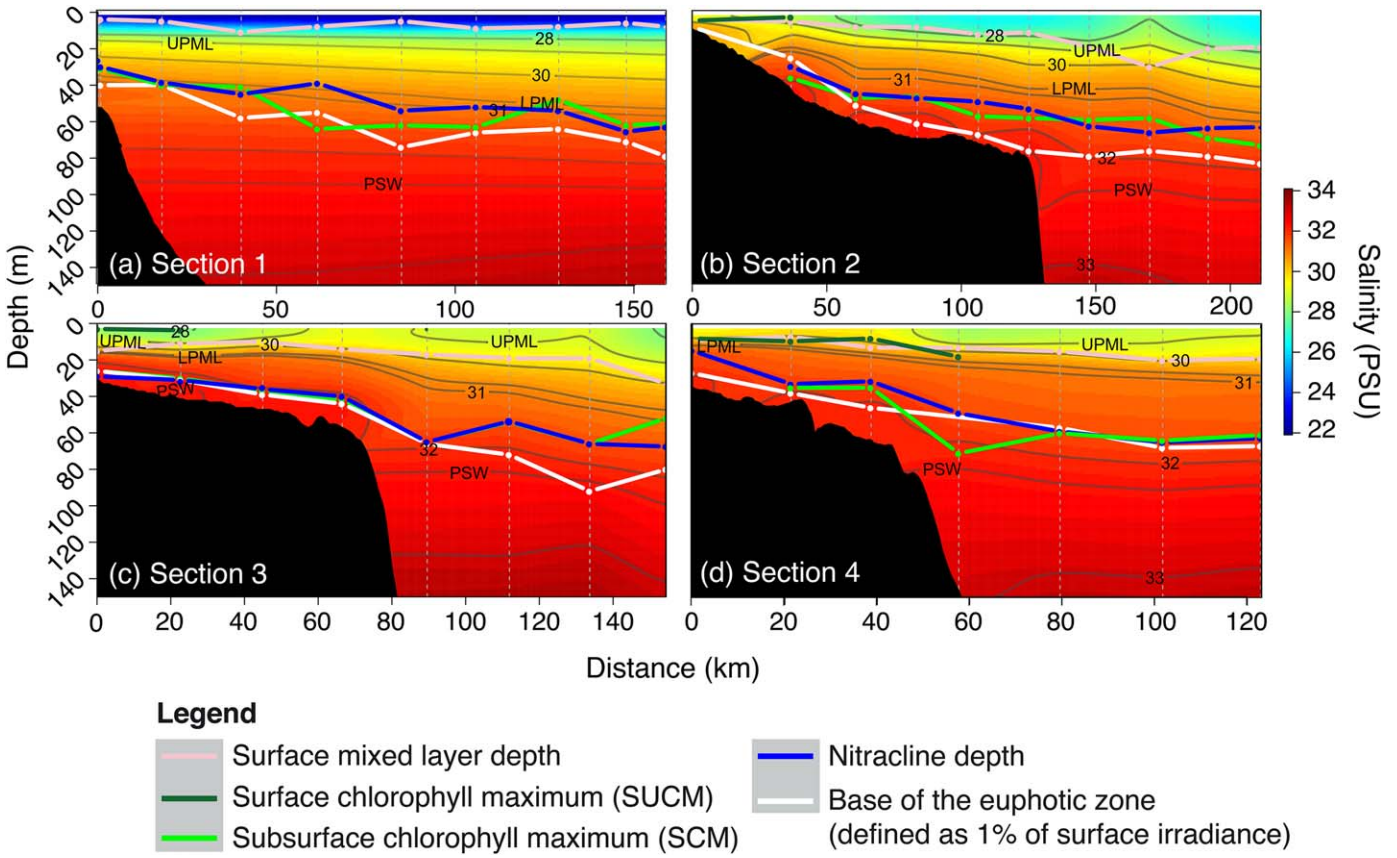

Fig. 2. Salinity along four sections from the continental shelf to the deep basin of the Beaufort Sea (*see* Fig. 1 for the section locations). The black lines and the colored boxes represent the different water masses (*see* the characteristics of the water masses in Table 1). The purple, green, blue, and white lines show the depths of the surface mixed layer, of the surface (SUCM) and the subsurface (SCM) chlorophyll maximum, of the nitracline and of the base of the euphotic zone (defined as 1% of surface irradiance), respectively. The bathymetry is extracted from the International Bathymetric Chart of the Arctic Ocean (Jakobsson et al. 2012).

and Tremblay et al. 2008). The data collected from the four sections reveal four vertical features in phytoplankton vertical profiles: (1) a widespread SCM in oceanic waters ($\geq$ 50 m) also associated with low Chl *a* level (0.2–0.5 μg L^{-1}) (Fig. 3a), (2) a SCM also near the coast with high Chl *a* concentration ($>$ 1 μg L^{-1}) (Fig. 3b,c), (3) a weak SUCM at the surface (0.2–0.5 μg L^{-1}) at some oceanic stations (mainly within section 3; Fig. 3c); and (4) a SUCM associated with the surface mixed layer near the coast ($<$ 50 m) (Fig. 3d). This spatial variability was further used to define four domains as described in the following section.

On the continental shelf, subsurface intrusions of nitrate- and silicate-rich waters of Pacific origin (PSW) were observed along the four sections (Fig. 4) and coincided with a SCM characterized by high Chl *a* concentration (Fig. 3). However, the SCMs in the oceanic waters were generally located above the base of the euphotic zone (within the 1–10% of surface irradiance), which is not the case near the coast where the SCM is associated with lower light levels (Fig. 5b). Large inputs of suspended sediments and colored dissolved organic matter from the Mackenzie River are undoubtedly responsible for higher light attenuation through the water column in coastal waters (Doxaran et al. 2012; Matsuoka et al. 2012; Antoine et al. 2013). Indeed, this strong signature was revealed by high values of beam attenuation in coastal waters (data not shown, *see* Forest et al. 2014). This illustrates that late-summer SCMs in the Beaufort Sea may be driven primarily by nitrate availability instead of light conditions. In addition, coastal SCMs were associated with higher Chl *a* (up to $\approx$ 10 times more) than oceanic SCMs even if they were developing at lower irradiance (Fig. 3). Greater nitrate concentrations were also available to coastal SCMs on average (5 μmol L^{-1} vs. 3 μmol L^{-1} for coastal and oceanic SCMs, respectively). But most importantly, the coastal SCMs had access to much larger ammonium concentrations than at any other locations (Fig. 4). These results are consistent with those of Martin et al. (2012): (1) SCMs typically operate at sub-optimal irradiance; and (2) late-summer SCMs may rely at least equally on ammonium and nitrate to fuel their growth when light levels are low.

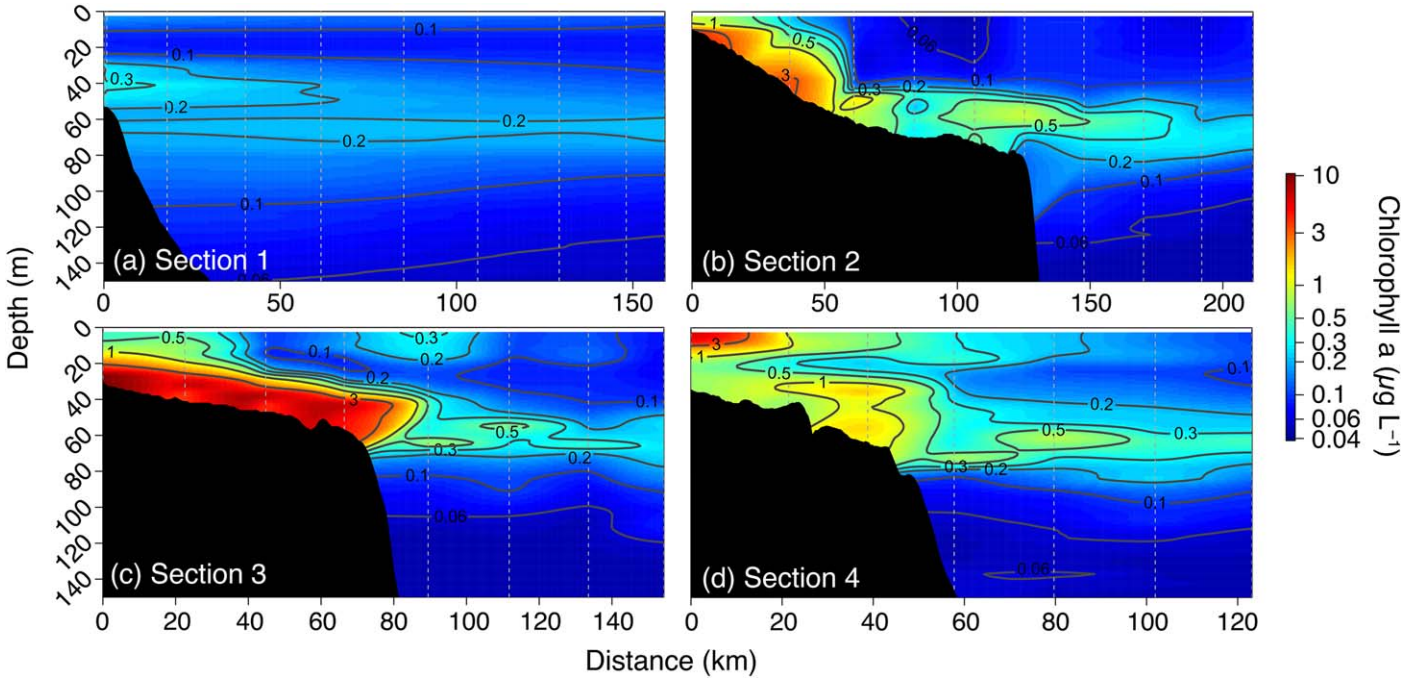

Fig. 3. In situ Chl *a* concentration along four transects from the continental shelf to the deep basin of the Beaufort Sea (*see* Fig. 1 for section locations). The black areas highlight the bathymetry.

The tight relation between SCMs and the nitracline depth indeed demonstrates that nitrate is a primary driver (Fig. 5a). Measurements of vertical nitrate flux for the Arctic Ocean are scarce and difficult to acquire (Bourgault et al. 2011; Randelhoff et al. 2015). Here, we use the steepness of the nitracline (Fig. 6) as a proxy to derive the vertical flux of nitrate (as described in Aksnes et al. 2007 and Omand and Mahadevan 2015). We observed a significant decrease in the steepness of the nitracline along the shelf-basin gradient (Fig. 6), which suggests that nitrate concentration increases rapidly with depth near the coast, while the vertical increase is more progressive offshore. In fact, the deep basin exhibited relatively strong vertical stratification, which maintained a gradual nitracline (*t*-test, $p < 0.0001$) and, presumably, a smaller vertical nitrate flux. It is thus likely that the magnitude of upward nitrate fluxes (shown here through the steepness of the nitracline) modulates the rate at which the SCM deepens and reaches its maximum depth. This vertical limit corresponds to the compensation light intensity below which net growth is no longer possible and a transition occurs toward net heterotrophy and associated communities.

Lateral advection of nitrate from offshore to the continental shelf (Fig. 4, *see* also Forest et al. 2014; Tremblay et al. 2014) is a crucial mechanism for injecting nitrate in the euphotic zone and consequently, sustaining a steep nitracline (i.e., high vertical nitrate flux). It has been shown to be related to upwelling-favorable winds (Carmack and Chapman 2003; Williams and Carmack 2008; Tremblay et al. 2011; Schulze and Pickart 2012; Pickart et al. 2013*b*). Interestingly, episodes of strong winds are not necessarily required to generate mild upwelling events of deep waters across the shelf break and over the shelf where they remain relatively confined to the bottom (Pickart et al. 2013; Forest et al. 2014). Such upwelling had apparently been taking place just before MALINA and its nutrient signature was still present at some locations over the shelf. This process has been shown to be important for maintaining productive diatoms-based SCMs and drive overall particulate carbon cycling over the continental shelf (*see* also Tolosa et al. 2013; Forest et al. 2014; Tremblay et al. 2014).

Phytoplankton community, nutrition, and primary production along the shelf/basin gradient of the Beaufort Sea

Three distinct groups of stations with different taxonomic compositions of protists emerge from a statistical analysis of similarities (Fig. 7 and Table 3), performed on samples collected at the surface and at the depth of SCM. Taxa characterizing each station group and the percent occurrence of each station group within the four domains delineated from the vertical Chl *a* distribution are presented in Table 3 (*see* Table 1 for the definition of the four domains). Table 4 summarizes the environmental conditions and biological characteristics of these diverse domains of the Beaufort Sea (i.e., for consistency, only the stations with taxonomic inventories were selected). Our data reveal distinct ecological niches and remarkable diversity in terms of taxonomic composition

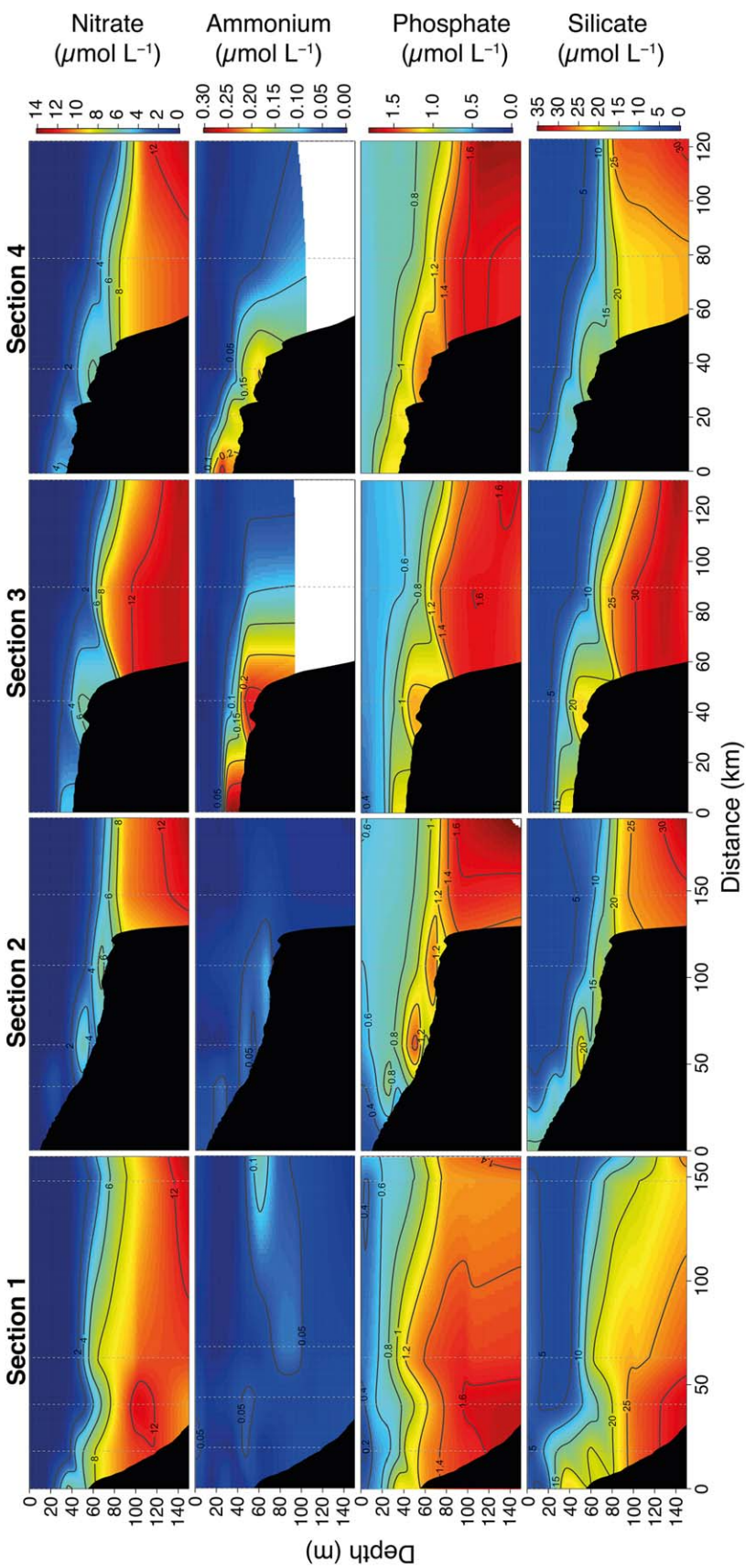

Fig. 4. Nitrate, ammonium, phosphate, and silicate concentrations along four transects from the continental shelf to the deep basin of the Beaufort Sea (*see* Fig. 1 for section locations). The black areas highlight the bathymetry.

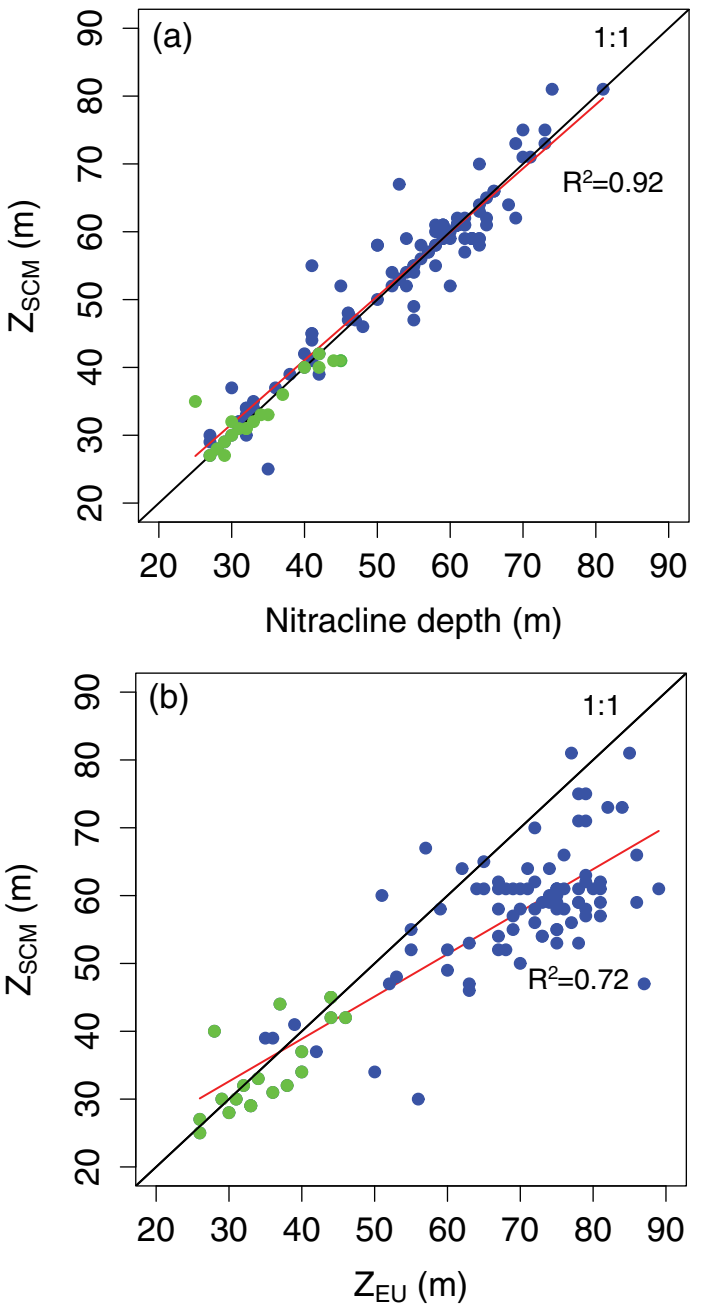

Fig. 5. Scatterplots of (**a**) the nitracline depth and (**b**) the euphotic zone depth (Z_{EU}, defined as 1% of surface irradiance) vs. the subsurface Chl *a* maximum depth (Z_{SCM}). Green and blue symbols represent coastal (< 50 m) and oceanic (≥ 50 m) stations, respectively. Black line represents perfect agreement, and red line represents the linear regression.

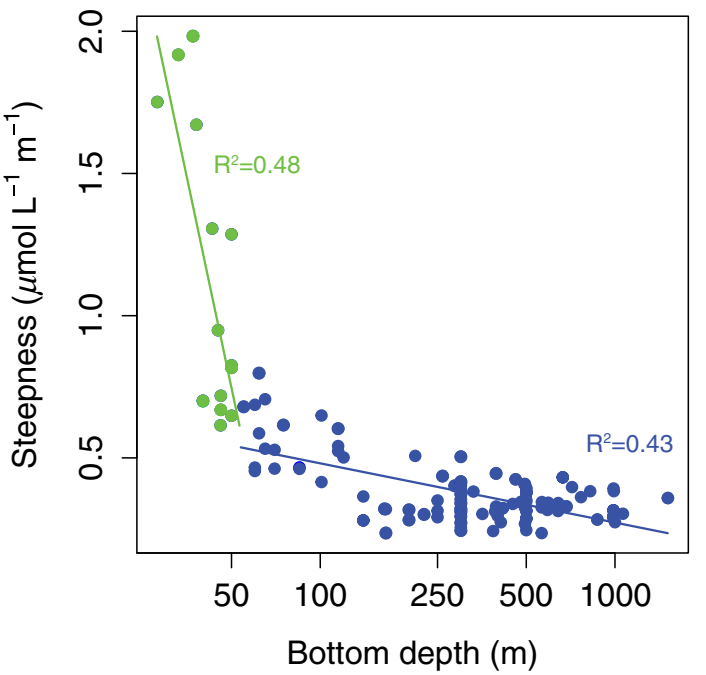

Fig. 6. Scatterplot of the steepness of the nitracline vs. the bottom depth, when a subsurface Chl *a* maximum (SCM) was detected. Green and blue symbols represent coastal (< 50 m) and oceanic (≥ 50 m) stations, respectively. Green and blue lines represent the linear regression for coastal and oceanic stations, respectively.

in the three station groups identified by the nMDS (Fig. 7 and detailed in Table 3), in agreement with the different vertical features described in the previous section. Group 1, the productive community (high Chl *a*; mean 2.41 μg L^{-1}), includes samples collected in coastal waters (67% and 100% of UC and SC samples, respectively). Group 2, the low productive community (low Chl *a*; mean 0.23 μg L^{-1}), is made of samples collected in oceanic waters (i.e., 21% and 100% of UO and SO samples, respectively). Finally, Group 3, the very low productive community (near-zero Chl *a*; mean 0.09 μg L^{-1}), combines samples from both coastal and oceanic waters (i.e., 33% and 79% of UC and UO samples, respectively). From the analysis of similarities, one particular station from the Group 1, located near the Mackenzie River delta, displayed a unique taxonomic composition and is discussed apart.

Group 1: Productive phytoplankton communities in coastal waters

The low salinity of surface waters (i.e., upper polar mixed layer [UPML] and lower polar mixed layer [LPML] in Fig. 2; UC and UO in Table 4), originating from both river discharge and melting sea ice, generates a strong vertical density gradient within the upper 10–20 m of the water column. In this surface mixed layer, a marked latitudinal transition in the taxonomic composition of protists (i.e., from large to small cells) was observed between coastal and oceanic waters (UC and UO, respectively in Table 3 and Fig. 7). However, most coastal stations did not show any taxonomical dissimilarities between the surface and subsurface (UC and SC, *see* Table 3) despite pronounced vertical gradients in physical and chemical properties (e.g., salinity, light, nitrate availability) (Table 4 and Figs. 2–4).

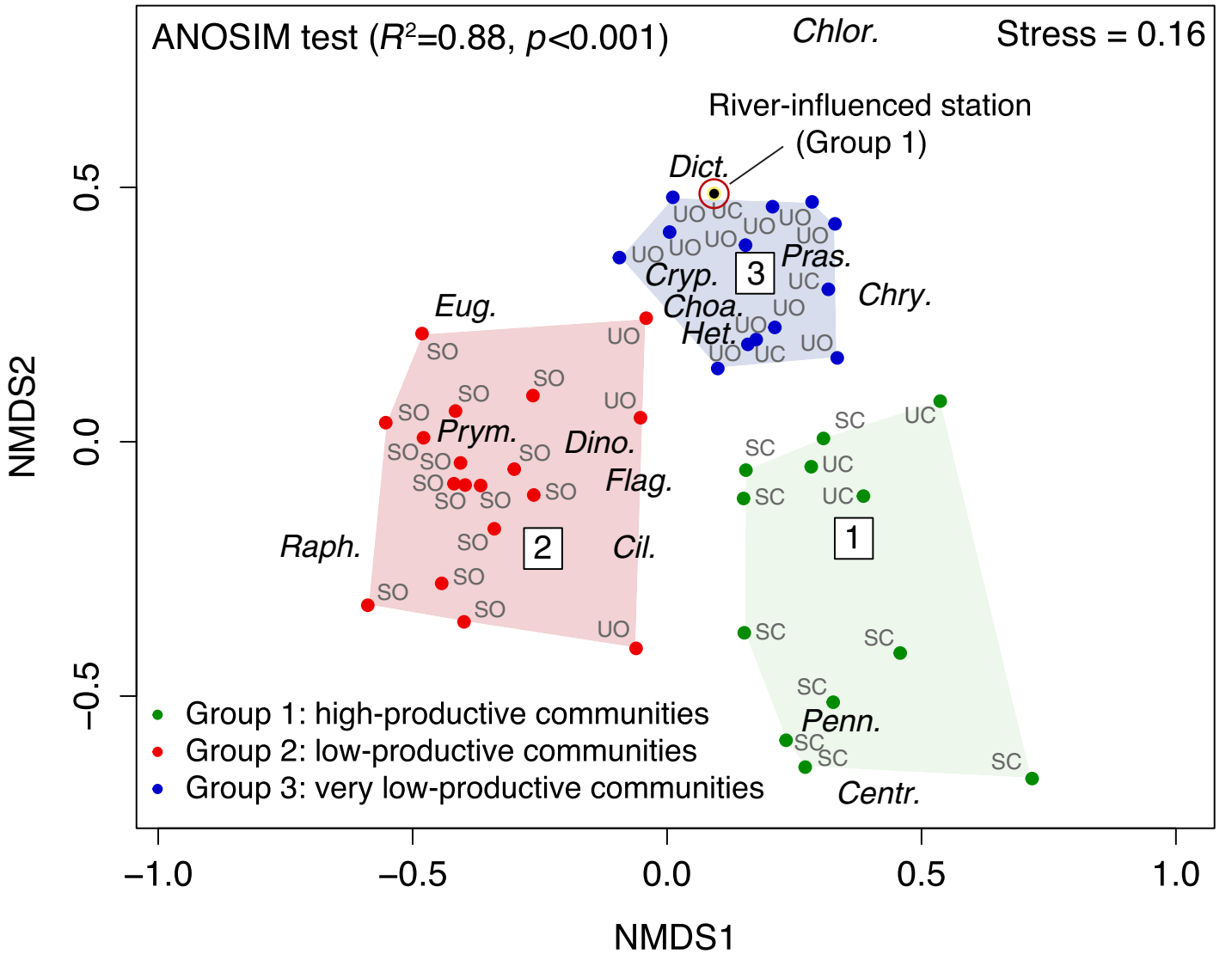

Fig. 7. Two-dimensional nMDS of 44 stations in the Beaufort Sea. The three groups of stations with taxonomically similar protist composition, as determined with the group-average clustering, are superimposed on the MDS. *Centr.*, centric diatoms; *Chlor.*, chlorophytes; *Choa.*, choanoflagellates; *Chrys.*, chrysophytes; *Cil.*, ciliates; *Crypt.*, cryptophytes; *Dict.*, dictyophytes; *Dino.*, dinoflagellates; *Eug.*, euglenophytes; *Flag.*, unidentified flagellates; *Het.*, heterotrophic groups; *Penn.*, pennate diatoms; *Pras.*, prasinophytes; *Prym.*, prymnesiophytes; *Raph.*, raphidophytes; UC, upper surface coastal water; SC, lower subsurface coastal water at the depth of SCM; UO, upper surface oceanic water; SO, lower subsurface oceanic water at the depth of SCM.

Surface communities from Group 1 (mainly UC) exhibited a high dominance of centric (mainly *Thalassiosira nordenskioeldii)* and pennate (i.e., *Pseudo-nitzschia* spp.) diatoms. This was the dominating community on the inner and mid-shelf, including the river-influenced station. The production and accumulation of large cells at the surface are likely related to direct allochthonous inputs of riverine nutrients and especially the indirect nitrogen supply resulting from intense recycling prevailing in the shallow surface mixed layer (i.e., from labile dissolved organic nitrogen [DON] and N_2 fixation) (Blais et al. 2012; Shen et al. 2012; Tremblay et al. 2014). Although ammonium concentrations were apparently low at the surface near the coast (UC, Fig. 8c), the high ammonium uptake rate of UC communities suggests that either they were primarily supported by nitrogen recycling, or that bacteria contributed actively to ammonium uptake in this environment, or a combination of both (Fig. 9c). The potential association between diatoms and regenerated production contrasts with the biogeochemical paradigm that typically relates large cells to nitrate-driven new production (Malone 1980). Hence, it appears that bacteria were responsible for a substantial fraction of the nitrogen uptake within our study cf. Kirchman and Wheeler (1998), especially near the coast. This would be consistent with Ortega-Retuerta et al. (2012) who reported elevated bacterial abundance and bacterial production rates over the shelf during MALINA in

Table 3. Breakdown of similarities within groups of stations into contributions (%) from each taxonomic division of protists. The percent number of stations from each domain that are present in each group is also presented as occurrence (%). Only the contributions of protist taxonomic divisions > 5% are presented. The main species and their size range of each taxonomic division are listed. Note that *Chaetoceros gelidus* and *Thalassiosira nordenskioeldi* are chain-forming species, that *Dinobryon balticum* is forming colonies and that *Calliacantha natans*, *C. longicaudata*, and chrysophytes possess a lorica. UC, upper surface coastal water; SC, lower subsurface coastal water at the depth of SCM; UO, upper surface oceanic water; SO, lower subsurface oceanic water at the depth of SCM; *n* = number of stations.

	Group 1 High-productive communities (mean 2.41 μg Chl *a* L^{-1})	**Group 2 Low-productive communities (mean 0.23 μg Chl *a* L^{-1})**	**Group 3 Very low-productive communities (mean 0.09 μg Chl *a* L^{-1})**	**River-influenced station (Group 1) (0.48 μg Chl *a* L^{-1})**
Taxonomic groups of protist (contributions (%) from each taxonomic division)				
Centric diatoms	95	9	—	66
Chaetoceros gelidus; 5–14 μm	✓	✓		✓
Thalassiosira nordenskioeldii; 11–41 μm	✓	✓		✓
Choanoflagellates	—	—	12	—
Calliacantha natans; cell length 7.2–24 μm, lorica length 28–43 μm			✓	
C. longicaudata; cell length 9.6–12 μm, lorica length 59–127 μm			✓	
Chrysophytes	—	—	7	—
Dinobryon spp.; cell 7–11 μm, lorica length 16–91 μm			✓	
D. balticum; cell 5–8.7 μm, lorica length 26–85 μm			✓	
Cryptophytes	—	7	—	5
Plagioselmis prolonga var. *nordica*; 6–12 μm		✓		✓
Hemiselmis spp.; 4–8.5 μm		✓		✓
Dictyophytes	—	—	6	5
Pseudopedinella spp. 2–5 μm & 5–10 μm			✓	✓
Dinoflagellates	—	17	13	10
Gymnodinium/*Gyrodinium* spp.; 10–20 μm; 20–50 μm		✓	✓	
G. galeatum; 17–26 μm		✓	✓	
H. rotundata; 7.2–17 μm				✓
Prasinophytes	—	—	13	—
Pyramimonas spp.; 2–5 μm & 5–10 μm			✓	
Prymnesiophytes	—	18	8	—
Chrysochromulina spp.; 2–5 μm & 5–10 μm		✓	✓	
Raphidophytes	—	6	—	—
Chattonella spp.; 30–50 μm		✓		
Heterosigma cf. *akashiwo*; 10–18 μm		✓		
Unidentified flagellates	—	34	29	6
Domains (Percent number (%) of stations from each domain that are present in each group of protist)				
UC (*n* = 6)	67	—	33	—
SC (*n* = 9)	100	—	—	—
UO (*n* = 14)	—	21	79	—
SO (*n* = 15)	—	100	—	—

association with riverine organic matter and warmer waters. Assuming that a typical C : N molar ratio of ~ 7 could be used to determine the actual proportion of carbon to nitrogen uptake rate by phytoplankton in the Beaufort Sea (Tremblay et al. 2008), this implies that at least 84–94% of the total nitrogen uptake near the coast was due to bacteria. This elevated range is above those measured in a non-river influenced Arctic sea (44–78%) by Fouilland et al. (2007),

Table 4. Physical, chemical, and biological variables, and the uptake and regeneration rates (mean ± SD) in the four distinct domains of the Beaufort Sea: UC, upper surface coastal water; SC, lower subsurface coastal water at the depth of SCM; UO, upper surface oceanic water; SO, lower subsurface oceanic water at the depth of SCM. For consistency, only the stations with taxonomic inventories were selected. The results of the Kruskal–Wallis *H* and Chi-square tests between different domains for each variable are indicated. Identical letters depict domains without statistically significant differences between the input variables at the 95% level ($p < 0.05$), whereas different letters depict significant differences between domains. The codes of the Kruskal–Wallis *H* significance are: * $p < 0.01$, ** $p < 0.001$, *** $p < 0.0001$; NS, non significant.

	Coastal water (< 50 m)		Oceanic water (≥ 50 m)		Kruskal-Wallis *H*-test				
						Chi-square test (≤ 0.05)			
	UC Mean ± SD	SC Mean ± SD	UO Mean ± SD	SO Mean ± SD	*p*	UC	SC	UO	SO
A) Physical and biological variables									
Temperature (°C)	4.82 ± 0.68	−1.02 ± 0.22	2.45 ± 2.38	−1.13 ± 0.21	***	a	b	c	b
Salinity (PSU)	27.8 ± 1.84	31.6 ± 1.14	25.3 ± 2.46	31.5 ± 0.39	***	a,c	b	a	b,c
Beam attenuation (m^{-1})	1.00 ± 0.33	1.05 ± 0.53	0.68 ± 3.89	0.48 ± 0.01	***	a	a	a,b	b
Chl *a* ($\mu g\ L^{-1}$)	0.21 ± 0.14	3.32 ± 2.32	0.08 ± 0.03	0.25 ± 0.14	**	a,c	b	c	a
POC ($\mu mol\ L^{-1}$)	14.7 ± 5.4	22.1 ± 11.2	5.3 ± 4.1	2.6 ± 1.29	***	a	b	a,c	c
B) Chemical data (*see* Fig. 8)									
Nitrate ($\mu mol\ L^{-1}$)	0.02 ± 0.01	5.4 ± 2.28	0.01 ± 0.01	3.29 ± 2.86	***	a	b	a	b
Nitrite ($\mu mol\ L^{-1}$)	0.01 ± 0.01	0.1 ± 0.06	0.003 ± 0.003	0.07 ± 0.03	***	a	b	a	b
Ammonium ($\mu mol\ L^{-1}$)	0.02 ± 0.01	0.15 ± 0.14	0.01 ± 0.01	0.02 ± 0.01	NS				
Phosphate ($\mu mol\ L^{-1}$)	0.39 ± 0.07	1.2 ± 0.28	0.47 ± 0.19	1.02 ± 0.26	***	a	b	a	b
Silicate ($\mu mol\ L^{-1}$)	4.8 ± 2.54	21.45 ± 5.67	4.52 ± 2.15	9.89 ± 4.18	***	a	b	a	a,b
C) Uptake and regeneration rates (*see* Fig. 9)									
Carbon uptake ($nmol\ C\ L^{-1}\ d^{-1}$)	263 ± 108	230 ± 291	205 ± 238	29.1 ± 18.9	*	a	a,b	a,b	b
NO_3 uptake ($nmol\ N\ L^{-1}\ d^{-1}$)	64.9 ± 21.5	316 ± 367	14.0 ± 16.8	10 ± 7.66	**	a	a	b	b
NH_4 uptake ($nmol\ N\ L^{-1}\ d^{-1}$)	163 ± 73.8	234 ± 303	58.9 ± 69.1	11.0 ± 9.4	*	a	a	a,b	b
NH_4 regeneration ($nmol\ N\ L^{-1}\ d^{-1}$)	112.6 ± 45.0	85.6 ± 81.2	26.8 ± 50.5	8.44 ± 6.72	*	a	a,b	b,c	c

suggesting a stimulation of bacterial activity by organic matter from the Mackenzie River in the nearshore zone.

Similarly to coastal UC communities, subsurface assemblages near the coast were dominated (100% of the SC stations) by high Chl *a* concentration and by a high abundance of centric diatoms (mainly *Chaetoceros gelidus*; *see* Group 1 in Table 3 and Fig. 7). These accumulations of large cells were directly related to local phytoplankton production at the nitracline depth (Forest et al. 2014; Tremblay et al. 2014; Coupel et al. 2015*a*). The coastal SCM communities were associated with relatively high ambient nutrient concentrations (Fig. 8) and much greater nitrate uptake rates in comparison with the coastal SUCMs (Fig. 9b,c), although the actual contribution of bacteria to nitrate and ammonium uptake remains uncertain. The range of uptake rates of ammonium below the surface layer in the coastal environment was large and overlapped with the range of nitrate uptake rates (Table 4). This reflects the importance of ammonium production by zooplankton excretion and microbial ammonification on the shelf (Forest et al. 2014; Tremblay et al. 2014), leading to a greater accumulation of ammonium at depth than in the surface mixed layer (Figs. 4, 8c). In this setting, nitrate uptake below the surface in the coastal region amounted to 40–60% of total nitrogen uptake (Table 4), a proportion approximatively twice greater than at the surface. Assuming that this proportion also represents the ratio of new to total primary production (i.e., despite the uncertainties related to nitrogen uptake by bacteria), the results suggest that the potential for carbon export was higher for coastal SCMs than for SUCMs. Indeed, the overwhelming dominance of large and fast-growing diatoms in the phytoplankton assemblage of the SC communities on the shelf (Table 3) is consistent with the high upward fluxes of nitrate, phosphate and silicate inferred from the steep nutricline.

Taxonomical similarity between most of the surface and subsurface phytoplankton communities near the coast suggests that the same ecological niche prevailed throughout this environment despite the large vertical gradients in salinity, light, phosphate, and silicate. The primary driver of this similarity thus appears to be the dissolved nitrogen inventory (either nitrate or ammonium) rather than the aforementioned factors. It may be also attributed to potential settling of large particles, including large diatoms cells. A remaining fraction of UC communities was nevertheless classified as

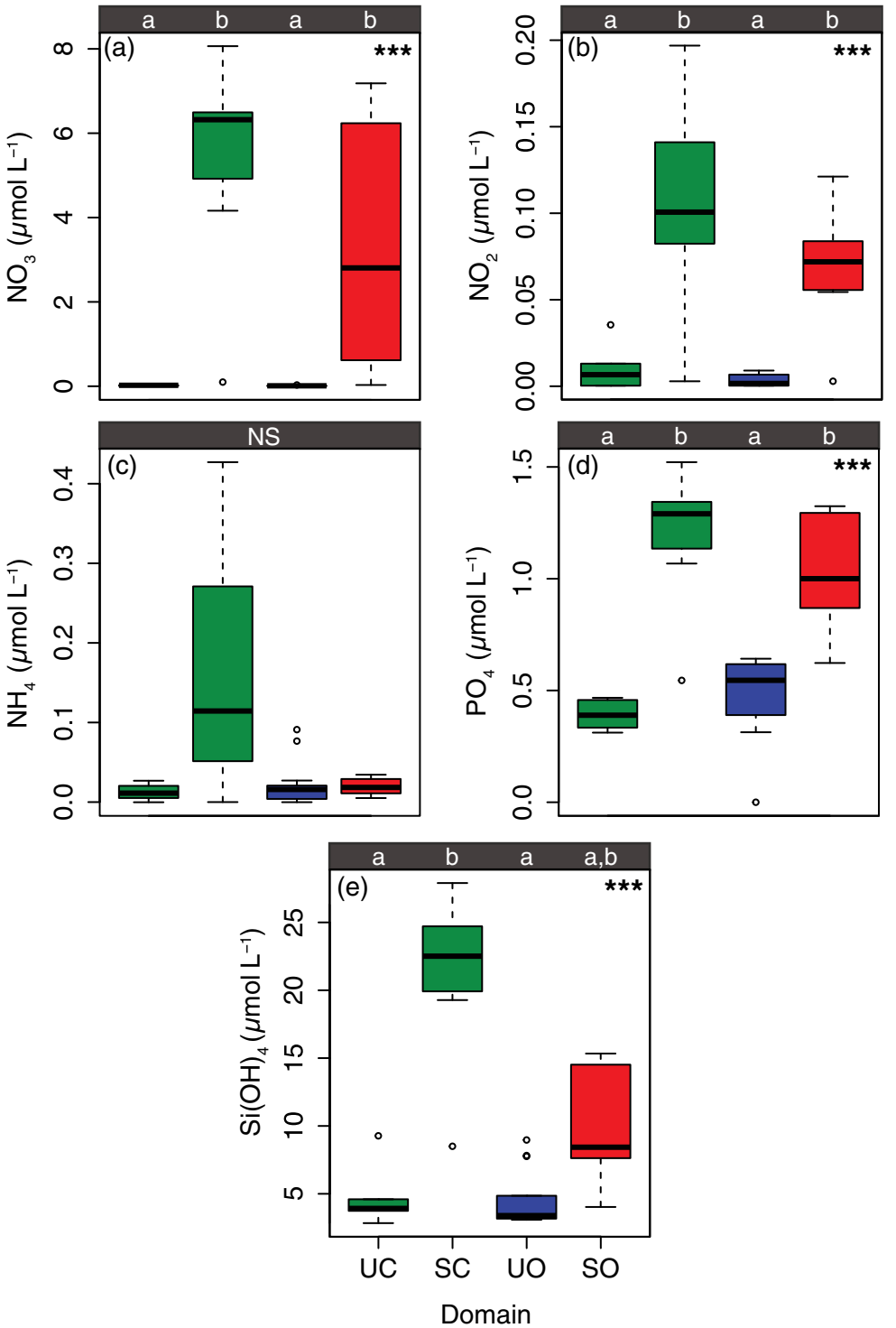

Fig. 8. Box plots of the domains (UC, SC, UO, SO; x axis) against their corresponding nutrient concentrations (y axis) ((**a**): nitrate, NO_3; (**b**): nitrite, NO_2; (**c**): ammonium, NH_4; (**d**): phosphate, PO_4, and (**e**): silicate, $Si(OH)_4$). For consistency, only the stations with taxonomic inventories were selected following the four distinct domains: UC, upper surface coastal water; SC, lower subsurface coastal water at the depth of SCM; UO, upper surface oceanic water; SO, lower subsurface oceanic water at the depth of SCM. The line in the middle of each box represents the region median. The top and bottom limits of each box are the 25th and 75th percentiles, respectively. The lines extending above and below each box, i.e., whiskers, represent the full range of non-outlier observations for each variable beyond the quartile range. Black circles (°) are observations that have been classified as outliers. The results of the Kruskal–Wallis *H* and Chi-square tests between different domains for each variable are shown in figures (**a**–**e**). Identical letters depict domains without statistically significant differences between the climatological input variables at the 95% level ($p < 0.05$), whereas different letters depict significant differences between domains. The codes of the Kruskal–Wallis *H* significance are: * $p < 0.01$; ** $p < 0.001$; *** $p < 0.0001$; NS, non significant.

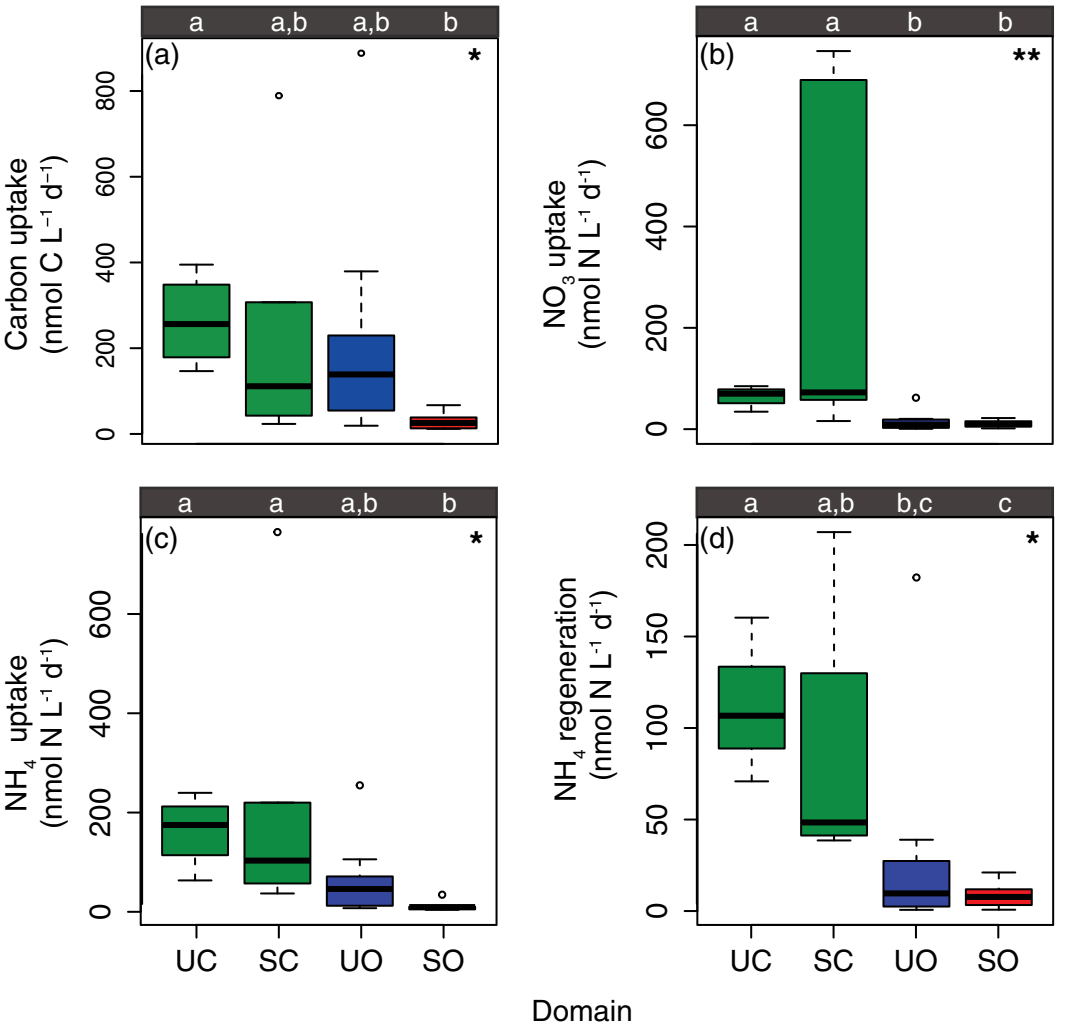

Fig. 9. Box plots of the domains (UC, SC, UO, SO; x axis) against their corresponding rate measurements (y axis) ((**a**): dissolved inorganic carbon uptake rate, (**b**): NO_3 uptake rate, (**c**): NH_4 uptake rate, and (**d**): NH_4 regeneration rate). For consistency, only the stations with taxonomic inventories were selected following the four distinct domains: UC, upper surface coastal water; SC, lower subsurface coastal water at the depth of SCM; UO, upper surface oceanic water; SO, lower subsurface oceanic water at the depth of SCM. The line in the middle of each box represents the region median. The top and bottom limits of each box are the 25th and 75th percentiles, respectively. The lines extending above and below each box, i.e., whiskers, represent the full range of non-outlier observations for each variable beyond the quartile range. Black circles (°) are observations that have been classified as outliers. The results of the Kruskal–Wallis *H* and Chi-square tests between different domains for each variable are shown in figures (**a**–**d**). Identical letters depict domains without statistically significant differences between the input variables at the 95% level ($p < 0.05$), whereas different letters depict significant differences between domains. The codes of the Kruskal–Wallis *H* significance are: * $p < 0.01$; ** $p < 0.001$.

part of Group 3 (dominated by prasinophytes and other small mixotrophs/heterotrophs, as discussed below). This suggests that a fraction of the coastal assemblages was already in an advanced phenological stage, consistent with our sampling taking place during a late summer period generally characterized by low production following the exhaustion of nitrate in the surface layer.

Group 2: Low-productive phytoplankton communities in oceanic waters

The stations that fall within Group 2 were all located in the oceanic waters and were generally characterized by low Chl *a* concentrations (i.e., mean 0.23 μg L^{-1}) at the surface (UO) or at the depth of the SCM (SO). The taxonomic composition of these oceanic SUCMs (21% of the UO stations) and SCMs (100% of SO stations) (Table 3 and Fig. 7), which differs drastically from those near the coast (i.e., UC and SC stations from Group 1), exhibits a dominance of unidentified flagellates, including a high abundance of small prymnesiophytes (*Chrysochromulina* spp. of 2–5 μm and 5–10 μm) and dinoflagellates (*Gymnodinium*/*Gyrodinium* spp. and *Gymnodinium galeatum*).

Primary production (i.e., carbon uptake) within SO communities and the uptake of nitrate and ammonium in the oceanic domain were all much lower than within the coastal

environments (Fig. 9), presumably reflecting the lower upward fluxes of nitrate based on the steepness of the nitracline (Fig. 6) as well as much less ammonium regeneration off the coast (i.e., less zooplankton and microbial activity). On the one hand, these results illustrate that low nitrogen uptake is indeed a synonym of low primary production and a key factor shaping the phytoplankton assemblage at a given location in the Beaufort Sea. Conversely, they strongly contrast with the relatively high ambient concentrations of nitrate, phosphate and silicate available to SO communities (Figs. 4, 8), the greater light levels at the SCM depth (1–10%; Fig. 5b), and the relatively high nitrate to total nitrogen uptake ratio shown for oceanic SCMs (0.5 on the average and up to 0.8 in some cases; Fig. 9). These characteristics of the SO environments and oceanic SCMs would be expected to correspond with communities showing a similar assemblage than on the shelf with a dominance of large cells, such as diatoms, but our results show otherwise.

Beyond the large nutrient pool available to SO communities, the large difference in the carbon fixation rate between the coastal and oceanic phytoplankton communities at the SCMs appears to be closely related to a stronger vertical stratification and gentler slope of the nitracline in the oceanic domain (i.e., lower vertical nitrate flux). It seems that light availability may not be the main limiting factor for phytoplankton growth at the SCM depth, since the presence of two distinct phytoplankton communities are observed both at the base of the euphotic zone over the continental shelf (i.e., group 1) and in the deep basin (group 2; Figs. 2, 3, 5b, 7). It is noteworthy that the depth of the SCM for both phytoplankton assemblages is located at the nitracline (Figs. 2, 5a) such that significant differences in vertical nitrate flux may determine differences in taxonomic composition. The steeper slope of the nitracline near the coast is presumably related to both a shallow water column and a shallow nitracline, which make possible a more effective turbulent mixing by wind and tides. These results support the important role of vertical nitrate flux in regulating phytoplankton composition and productivity as described in previous studies, carried out in several coastal and oceanic waters in the global ocean (Lewis et al. 1986; Sharples et al. 2001; Hales et al. 2005, 2009; Rippeth et al. 2009; Li et al. 2012).

The relatively elevated nitrogen uptake rates for oceanic communities in comparison to the carbon fixation rates measured in the offshore environment (Table 4) underscore again that bacteria were key contributors to nitrogen uptake across the shelf-basin gradient. Using a typical C : N ratio of ~ 7 (Tremblay et al. 2008) to estimate the actual nitrogen uptake rate by phytoplankton off the shelf results in nitrogen assimilation by bacteria possibly cumulating to at least 60–80% of the (weak) total nitrogen uptake. Although still elevated, this illustrates the progressively lower impact of bacteria on nitrogen cycling as the marine ecosystem transits away from high riverine inputs of active microbes and dissolved organic carbon (Ortega-Retuerta et al. 2012). Indeed, these estimates of nitrogen uptake by bacteria for the basin environment are consistent with those of Fouilland et al. (2007) who measured that about 44–78% of the total nitrogen uptake was linked to bacteria in the Baffin Bay, a non-river influenced Arctic sea.

Group 3: Very low productive communities at the surface near the coast and offshore

Moving further away from the neritic zone impacted by riverine nutrients, strong haline stratification (i.e., maintained mainly by sea-ice meltwater) hampers vertical mixing and consequently, upward inorganic nutrient supply to the surface layer (Figs. 2, 4). These extreme conditions of oligotrophy (*see* Fig. 4) tend to strongly limit primary production, which is solely based on the activity of small phytoplankton cells associated with near-zero level of Chl *a* (i.e., mixotrophic and heterotrophic communities) as reflected in the taxonomic composition of Group 3 (*see* Table 3; Figs. 7, 9). Group 3 comprised 79% and 33% of the UO and UC stations, respectively. A further decrease in the nitrate to total nitrogen uptake ratio was also seen at the surface when moving from the coast to the basin (from 0.31 ± 0.07 to 0.19 ± 0.09; Table 3; Fig. 9), implying that surface protist communities and bacteria increasingly depend on nitrogen recycling for their development away from the shelf.

The near-absence of nitrate renders these communities reliant on nitrogen recycling, hence the light-mediated processes, such as photo-ammonification (i.e., photochemically production of ammonium from photosensitive DON), have been shown to be a non-negligible source of nitrogen and necessary for sustaining autotrophic and heterotrophic production in the surface layer during the MALINA expedition (Xie et al. 2012; Le Fouest et al. 2013). The bacterial production stimulated by fresh labile DON (Garneau et al. 2008; Ortega-Retuerta et al. 2013) also supports mixotrophic communities through the carbon assimilation mode (the prasinophyte *Pyramimonas* spp.; both 2–5 μm and 5–10 μm; *see* also Balzano et al. 2012 and Mckie-Krisberg and Sanders 2014) and indirectly, heterotrophic communities by grazing (principally the dinoflagellates *Gymnodinium/Gyrodinium* spp. and *G. galeatum*, and the ciliates *Lohmanniella oviformis* and *Strombidium* spp.; *see* also Sherr et al. 2009, 2013, and Ardyna et al. 2011).

The river-influenced station

On the inner shelf, there was one particular station located at the southernmost of section 2 (Fig. 1) that revealed a different upper community which was classified as having the characteristics of the Group 1, including some similarities with the Group 3 (Table 3 and Fig. 7). This shallow station had a brackish water signature (surface salinity at 27.3 Practical Salinity Unit (PSU)) due to its proximity from the Mackenzie River delta and was characterized by the presence of a SUCM only. The phytoplankton assemblage at this site

was dominated by centric diatoms as other coastal stations, but also displayed a high abundance of mesohaline dinoflagellates (*Heterocapsa rotundata*). The localized presence of such species on the inner shelf implies that mesohaline flagellates do not multiply on the shelf per se, but are rather transported by riverine waters into the nearshore environment.

Conclusions

The nature of phytoplankton functional groups (e.g., flagellate- vs. diatom-based systems) typically determine the potential for carbon transfer to higher trophic levels or for carbon export in the ocean (i.e., sinking of large cells such as diatoms) (Tremblay et al. 2009; Ardyna et al. 2011). At small spatial scales in the Beaufort Sea, the environmental complexity of the shelf-basin gradient allows the development of distinct ecological niches and high protist diversity in the euphotic zone (i.e., both horizontally and vertically). This observed protist diversity is supported additionally by the pigment signatures of phytoplankton communities, as revealed by Coupel et al. (2015*a*). In addition, vertical Chl *a* profiles appears to be implicitly related to phytoplankton community functioning, composition and structure, which remain critical to include for improving any satellite-derived phytoplankton proxies (i.e., phytoplankton biomass and productivity, and phytoplankton functional types; Babin et al. 2015; Lee et al. 2015). Here, we demonstrate that clear vertical and shelf-basin transitions in the relative magnitude of primary production emerge due to specific environmental forcing and distinct phytoplankton assemblages, underpinning the importance of the physical regime (i.e., turbulent mixing) and different nutritive strategies in surface/subsurface waters of the Beaufort Sea during oligotrophic summer conditions.

In the context of rapid environmental changes, an increasingly lengthy period of ice-free conditions and episodic wind-driven shelf-break upwelling will combine to promote diatom accumulations in the nearshore and over the continental shelf at a pan-Arctic scale (Nishino et al. 2011; Tremblay et al. 2011). These hotspots maintain a high autotrophic productivity and are crucial for marine Arctic ecosystems, locally and through the export of biological production during eddy migration toward the central Arctic (Watanabe et al. 2014). With the ongoing freshening, increased stratification and strengthening of the oligotrophic regime in the Western Arctic Ocean (McLaughlin and Carmack 2010; Coupel et al. 2015*b*), coastal hotspots of high autotrophic productivity may play an even more disproportionate role in supporting marine oceanic ecosystems as oases of fresh resources within a marine biome generally characterized by heterotrophic productivity (recycling) and low carbon transfer efficiency.

References

Aksenov, Y., S. Bacon, A. C. Coward, and N. P. Holliday. 2010. Polar outflow from the Arctic Ocean: A high resolution model study. J. Mar. Syst. **83**: 14–37. doi:10.1016/j.jmarsys.2010.06.007

Aksnes, D. L., M. D. Ohman, and P. Riviere. 2007. Optical effect on the nitracline in a coastal upwelling area. Limnol. Oceanogr. **52**: 1179–1187. doi:10.4319/lo.2007.52.3.1179

Aminot, A., and R. Kérouel. 2007. Dosage automatique des nutriments dans les eaux marines: Méthodes en flux continu. IFREMER.

Antoine, D., S. B. Hooker, S. Bélanger, A. Matsuoka, and M. Babin. 2013. Apparent optical properties of the Canadian Beaufort Sea - part 1: Observational overview and water column relationships. Biogeosciences **10**: 4493–4509. doi:10.5194/bg-10-4493-2013

Ardyna, M., M. Gosselin, C. Michel, M. Poulin, and J.-É. Tremblay. 2011. Environmental forcing of phytoplankton community structure and function in the Canadian High Arctic: Contrasting oligotrophic and eutrophic regions. Mar. Ecol. Prog. Ser. **442**: 37–57. doi:10.3354/meps09378

Ardyna, M., M. Babin, M. Gosselin, E. Devred, S. Bélanger, A. Matsuoka, and J.-É. Tremblay. 2013. Parameterization of vertical chlorophyll *a* in the Arctic Ocean: Impact of the subsurface chlorophyll maximum on regional, seasonal, and annual primary production estimates. Biogeosciences **10**: 4383–4404. doi:10.5194/bg-10-4383-2013

Ardyna, M., M. Babin, M. Gosselin, E. Devred, L. Rainville, and J.-É. Tremblay. 2014. Recent Arctic Ocean sea-ice loss triggers novel fall phytoplankton blooms. Geophys. Res. Lett. **41**: 6207–6212. doi:10.1002/2014GL061047

Arrigo, K. R., and G. L. Van Dijken. 2015. Continued increases in Arctic Ocean primary production. Prog. Oceanogr. **136**: 60–70. doi:10.1016/j.pocean.2015.05.002

Babin, M., S. Bélanger, I. Ellinsten, A. Forest, V. Le Fouest, T. Lacour, M. Ardyna, and D. Slagstad. 2015. Estimation of primary production in the Arctic Ocean using ocean colour remote sensing and coupled physical-biological models: Strengths, limitations and how they compare. Prog. Oceanogr. **139**: 197–220. doi:10.1016/j.pocean.2015.08.008

Balzano, S., P. Gourvil, R. Siano, M. Chanoine, D. Marie, S. Lessard, D. Sarno, and D. Vaulot. 2012. Diversity of cultured photosynthetic flagellates in the northeast Pacific and Arctic Oceans in summer. Biogeosciences **9**: 4553–4571. doi:10.5194/bg-9-4553-2012

Bérard-Therriault, L., M. Poulin, and L. Bossé. 1999. Guide d'identification du phytoplancton marin de l'estuaire et du golfe du Saint-Laurent incluant également certains protozoaires. Publ. spéc. Can. sci. halieut. aquat. **128**, 387 p. doi:10.1139/9780660960579

Blais, M., J.-É. Tremblay, A. D. Jungblut, J. Gagnon, J. Martin, M. Thaler, and C. Lovejoy. 2012. Nitrogen fixation and identification of potential diazotrophs in the

Canadian Arctic. Global Biogeochem. Cycles **26**: GB3022. doi:10.1029/2011gb004096

Blais, M., and others 2017. Contrasting interannual changes in phytoplankton productivity and community structure in the coastal Canadian Arctic Ocean. Limnol. Oceanogr. In press. doi:10.1002/lno.10581

Bourgault, D., C. Hamel, F. Cyr, J.-É. Tremblay, P. S. Galbraith, D. Dumont, and Y. Gratton. 2011. Turbulent nitrate fluxes in the Amundsen Gulf during ice-covered conditions. Geophys. Res. Lett. **38**: L15602. doi:10.1029/2011GL047936

Brown, Z. W., K. E. Lowry, M. A. Palmer, G. L. Van Dijken, M. M. Mills, R. S. Pickart, and K. R. Arrigo. 2015. Characterizing the subsurface chlorophyll *a* maximum in the Chukchi Sea and Canada Basin. Deep-Sea Res. Part II Top. Stud. Oceanogr. **118**: 88–104. doi:10.1016/j.dsr2.2015.02.010

Carmack, E. C., and R. W. Macdonald. 2002. Oceanography of the Canadian shelf of the Beaufort Sea: A setting for marine life. Arctic **55**: 29–45. doi:10.14430/arctic733

Carmack, E. C., and D. C. Chapman. 2003. Wind-driven shelf/basin exchange on an Arctic shelf: The joint roles of ice cover extent and shelf-break bathymetry. Geophys. Res. Lett. **30**: 1778. doi:10.1029/2003gl017526

Carmack, E. C., R. W. Macdonald, and S. Jasper. 2004. Phytoplankton productivity on the Canadian Shelf of the Beaufort Sea. Mar. Ecol. Prog. Ser. **277**: 37–50. doi:10.3354/meps277037

Citta, J. J., and others. 2015. Ecological characteristics of core-use areas used by Bering–Chukchi–Beaufort (BCB) bowhead whales, 2006–2012. Prog. Oceanogr. **136**: 201–222. doi:10.1016/j.pocean.2014.08.012

Clarke, K. R. 1993. Non-parametric multivariate analyses of changes in community structure. Aust. J. Ecol. **18**: 117–143. doi:10.1111/j.1442-9993.1993.tb00438.x

Clarke, K. R., and R. M. Warwick. 2001. A further biodiversity index applicable to species lists: Variation in taxonomic distinctness. Mar. Ecol. Prog. Ser. **216**: 265–278. doi:10.3354/meps216265

Codispoti, L. A., V. Kelly, A. Thessen, P. Matrai, S. Suttles, V. Hill, M. Steele, and B. Light. 2013. Synthesis of primary production in the Arctic Ocean: III. Nitrate and phosphate based estimates of net community production. Prog. Oceanogr. **110**: 126–150. doi:10.1016/j.pocean.2012.11.006

Conlan, K., E. Hendrycks, A. Aitken, B. Williams, S. Blasco, and E. Crawford. 2013. Macrofaunal biomass distribution on the Canadian Beaufort Shelf. J. Mar. Syst. **127**: 76–87. doi:10.1016/j.jmarsys.2013.07.013

Coupel, P., A. Matsuoka, D. Ruiz-Pino, M. Gosselin, D. Marie, J.-É. Tremblay, and M. Babin. 2015*a*. Pigment signatures of phytoplankton communities in the Beaufort Sea. Biogeosciences **12**: 991–1006. doi:10.5194/bg-12-991-2015

Coupel, P., D. Ruiz-Pino, M. A. Sicre, J. F. Chen, S. H. Lee, N. Schiffrine, H. L. Li, and J. C. Gascard. 2015*b*. The impact of freshening on phytoplankton production in the Pacific Arctic Ocean. Prog. Oceanogr. **131**: 113–125. doi:10.1016/j.pocean.2014.12.003

Doxaran, D., J. Ehn, S. Bélanger, A. Matsuoka, S. Hooker, and M. Babin. 2012. Optical characterisation of suspended particles in the Mackenzie River plume (Canadian Arctic Ocean) and implications for ocean colour remote sensing. Biogeosciences **9**: 3213–3229. doi:10.5194/bg-9-3213-2012

Forest, A., and others. 2011. Biogenic carbon flows through the planktonic food web of the Amundsen Gulf (Arctic Ocean): A synthesis of field measurements and inverse modeling analyses. Prog. Oceanogr. **91**: 410–436. doi:10.1016/j.pocean.2011.05.002

Forest, A., and others. 2014. Synoptic evaluation of carbon cycling in Beaufort Sea during summer: Contrasting river inputs, ecosystem metabolism and air–sea CO2 fluxes. Biogeosciences **11**: 2827–2856. doi:10.5194/bg-11-2827-2014

Fouilland, E., M. Gosselin, R. B. Rivkin, C. Vasseur, and B. Mostajir. 2007. Nitrogen uptake by heterotrophic bacteria and phytoplankton in Arctic surface waters. J. Plankton Res. **29**: 369–376. doi:10.1093/plankt/fbm022

Garneau, M.-È., M. Gosselin, B. Klein, J.-È. Tremblay, and E. Fouilland. 2007. New and regenerated production during a late summer bloom in an Arctic polynya. Mar. Ecol. Prog. Ser. **345**: 13–26. doi:10.3354/meps06965

Garneau, M.-È., S. Roy, C. Lovejoy, Y. Gratton, and W. F. Vincent. 2008. Seasonal dynamics of bacterial biomass and production in a coastal arctic ecosystem: Franklin Bay, western Canadian Arctic. J. Geophys. Res. **113**: C07S91. doi:10.1029/2007JC004281

Grebmeier, J. M., W. O. J. Smith, and R. J. Conover. 1995. Biological processes on arctic continental shelves: Ice-ocean biotic interactions. Am. Geophys. Union. 231–261. doi:10.1029/CE049p0231

Hales, B., J. N. Moum, P. Covert, and A. Perlin. 2005. Irreversible nitrate fluxes due to turbulent mixing in a coastal upwelling system. J. Geophys. Res. **110**: C10S11. doi:10.1029/2004JC002685

Hales, B., D. Hebert, and J. Marra. 2009. Turbulent supply of nutrients to phytoplankton at the New England shelf break front. J. Geophys. Res. **114**: C05010. doi:10.1029/2008JC005011

Harrison, W. G., and G. F. Cota. 1991. Primary production in polar waters: Relation to nutrient availability. Polar Res. **10**: 87–104. doi:10.3402/polar.v10i1.6730

Hill, V., M. Ardyna, S. H. Lee, and D. Varela. 2017. Decadal trends in phytoplankton production in the Pacific Arctic Region from 1950 to 2012. Deep-Sea Res. Part II Top. Stud. Oceanogr. In press. doi:10.1016/j.dsr2.2016.12.015

Holmes, R. M., A. Aminot, R. Kérouel, B. A. Hooker, and B. J. Peterson. 1999. A simple and precise method of measuring ammonium in marine and freshwater ecosytems. Can. J. Fish. Aquat. Sci. **56**: 1801–1808. doi:10.1139/cjfas-56-10-1801

Ji, R., M. Jin, and Ø. Varpe. 2012. Sea ice phenology and timing of primary production pulses in the Arctic Ocean. Glob. Change Biol. **19**: 734–741. doi:10.1111/gcb.12074

Kahru, M., V. Brotas, M. Manzano-Sarabio, and B. G. Mitchell. 2010. Are phytoplankton blooms occurring earlier in the Arctic? Glob. Change Biol. **17**: 1733–1739. doi:10.1111/j.1365-2486.2010.02312.x

Kirchman, D. L., and P. A. Wheeler. 1998. Uptake of ammonium and nitrate by heterotrophic bacteria and phytoplankton in the sub-Arctic Pacific. Deep-Sea Res. Part I Oceanogr. Res. Pap. **45**: 347–365. doi:10.1016/S0967-0637(97)00075-7

Kirkwood, D. S. 1992. Stability of solutions of nutrients salts during storage. Mar. Chem. **38**: 151–164. doi:10.1016/0304-4203(92)90032-6

Laws, E. 1984. Isotope dilution models and the mystery of the vanishing ^{15}N. Limnol. Oceanogr. **29**: 379–386. doi:10.4319/lo.1984.29.2.0379

Le Fouest, V., B. Zakardjian, H. Xie, P. Raimbault, F. Joux, and M. Babin. 2013. Modeling plankton ecosystem functioning and nitrogen fluxes in the oligotrophic waters of the Beaufort Sea, Arctic Ocean: A focus on light-driven processes. Biogeosciences **10**: 4785–4800. doi:10.5194/bg-10-4785-2013

Lee, Y. J., and others. 2015. An assessment of phytoplankton primary productivity in the Arctic Ocean from satellite ocean color/in situ chlorophyll-a-based models. J. Geophys. Res. **120**: 6508–6541. doi:10.1002/2015JC011018

Lewis, M. R., W. G. Harrison, N. S. Oakey, D. Hebert, and T. Platt. 1986. Vertical nitrate fluxes in the oligotrophic ocean. Science **234**: 870–873. doi:10.1126/science.234.4778.870

Li, Q. P., P. J. S. Franks, M. D. Ohman, and M. R. Landry. 2012. Enhanced nitrate fluxes and biological processes at a frontal zone in the southern California current system. J. Plankton Res. **34**: 790–801. doi:10.1093/plankt/fbs006

Li, W. K. W., F. A. McLaughlin, C. Lovejoy, and E. C. Carmack. 2009. Smallest algae thrive as the Arctic Ocean freshens. Science **326**: 539. doi:10.1126/science.1179798

Lovejoy, C. 2014. Changing views of Arctic protists (marine microbial eukaryotes) in a changing Arctic. Acta Protozool. **53**: 91–100. doi:10.4467/16890027ap.14.009.1446

Lund, J. W. G., C. Kipling, and E. D. Le Cren. 1958. The inverted microscope method of estimating algal numbers and the statistical basis of estimations by counting. Hydrobiologia **11**: 143–170. doi:10.1007/BF00007865

Malone, T. C. 1980. Algal size, p. 433–463. *In* I. Morris [ed.], The physiological ecology of phytoplankton. Blackwell Scientific Publications.

Martin, J., and others. 2010. Prevalence, structure and properties of subsurface chlorophyll maxima in Canadian Arctic waters. Mar. Ecol. Prog. Ser. **412**: 69–84. doi:10.3354/meps08666

Martin, J., J.-É. Tremblay, and N. M. Price. 2012. Nutritive and photosynthetic ecology of subsurface chlorophyll maxima in Canadian Arctic waters. Biogeosciences **9**: 5353–5371. doi:10.5194/bg-9-5353-2012

Martini, K. I., P. J. Stabeno, C. Ladd, P. Winsor, T. J. Weingartner, C. W. Mordy, and L. B. Eisner. 2016. Dependence of subsurface chlorophyll on seasonal water masses in the Chukchi Sea. J. Geophys. Res. **121**: 1755–1770. doi:10.1002/2015JC011359

Matsuoka, A., A. Bricaud, R. Benner, J. Para, R. Sempéré, L. Prieur, S. Bélanger, and M. Babin. 2012. Tracing the transport of colored dissolved organic matter in water masses of the Southern Beaufort Sea: Relationship with hydrographic characteristics. Biogeosciences **9**: 925–940. doi:10.5194/bg-9-925-2012

McKie-Krisberg, Z. M., and R. W. Sanders. 2014. Phagotrophy by the picoeukaryotic green alga *Micromonas*: Implications for Arctic Oceans. ISME J. **8**: 1953–1963. doi:10.1038/ismej.2014.16

McLaughlin, F. A., and E. C. Carmack. 2010. Deepening of the nutricline and chlorophyll maximum in the Canada Basin interior. Geophys. Res. Lett. **37**: L24602. doi:10.1029/2010gl045459

Michel, C., J. Hamilton, E. Hansen, D. Barber, M. Reigstad, J. Iacozza, L. Seuthe, and A. Niemi. 2015. Arctic Ocean outflow shelves in the changing Arctic: A review and perspectives. Prog. Oceanogr. **139**: 66–88. doi:10.1016/j.pocean.2015.08.007

Monier, A., J. Comte, M. Babin, A. Forest, A. Matsuoka, and C. Lovejoy. 2014. Oceanographic structure drives the assembly processes of microbial eukaryotic communities. ISME J. **9**: 990–1002. doi:10.1038/ismej.2014.197

Nishino, S., T. Kikuchi, M. Yamamoto-Kawai, Y. Kawaguchi, T. Hirawake, and M. Itoh. 2011. Enhancement/reduction of biological pump depends on ocean circulation in the sea-ice reduction regions of the Arctic Ocean. J. Oceanogr. **67**: 305–314. doi:10.1007/s10872-011-0030-7

Omand, M. M., and A. Mahadevan. 2015. The shape of the oceanic nitracline. Biogeosciences **12**: 3273–3287. doi:10.5194/bg-12-3273-2015

Ortega-Retuerta, E., and others. 2012. Carbon fluxes in the Canadian Arctic: Patterns and drivers of bacterial abundance, production and respiration on the Beaufort Sea margin. Biogeosciences **9**: 3679–3692. doi:10.5194/bg-9-3679-2012

Ortega-Retuerta, E., F. Joux, W. H. Jeffrey, and J. F. Ghiglione. 2013. Spatial variability of particle-attached and free-living bacterial diversity in surface waters from the Mackenzie River to the Beaufort Sea (Canadian Arctic). Biogeosciences **10**: 2747–2759. doi:10.5194/bg-10-2747-2013

Parsons, T., Y. Maita, and C. Lalli. 1984. A manual of chemical and biological methods for seawater analysis. Pergamon.

Pickart, R. S., L. M. Schulze, G. W. K. Moore, M. A. Charette, K. R. Arrigo, G. Van Dijken, and S. L. Danielson. 2013.

Long-term trends of upwelling and impacts on primary productivity in the Alaskan Beaufort Sea. Deep-Sea Res. Part I Oceanogr. Res. Pap. **79**: 106–121. doi:10.1016/j.dsr.2013.05.003

Poulin, M., N. Daugbjerg, R. Gradinger, L. Ilyash, T. Ratkova, and C. Von Quillfeldt. 2011. The pan-Arctic biodiversity of marine pelagic and sea-ice unicellular eukaryotes: A first-attempt assessment. Mar. Biodivers. **41**: 13–28. doi:10.1007/s12526-010-0058-8

Raimbault, P., G. Slawyk, B. Coste, and J. Fry. 1990. Feasibility of using an automated colorimetric procedure for the determination of seawater nitrate in the 0 to 100 nM range: Examples from field and culture. Mar. Biol. **104**: 347–351. doi:10.1007/BF01313277

Raimbault, P., W. Pouvesle, F. Diaz, N. Garcia, and R. Sempéré. 1999*a*. Wet-oxidation and automated colorimetry for simultaneous determination of organic carbon, nitrogen and phosphorus dissolved in seawater. Mar. Chem. **66**: 161–169. doi:10.1016/S0304-4203(99)00038-9

Raimbault, P., and others. 1999*b*. Carbon and nitrogen uptake and export in the equatorial Pacific at 150°W: Evidence of an efficient regenerated production cycle. J. Geophys. Res. **104**: 3341–3356. doi:10.1029/1998JC900004

Raimbault, P., and N. Garcia. 2008. Evidence for efficient regenerated production and dinitrogen fixation in nitrogen-deficient waters of the South Pacific Ocean: Impact on new and export production estimates. Biogeosciences **5**: 323–338. doi:10.5194/bg-5-323-2008

Randelhoff, A., A. Sundfjord, and M. Reigstad. 2015. Seasonal variability and fluxes of nitrate in the surface waters over the Arctic shelf slope. Geophys. Res. Lett. **42**: 3442–3449. doi:10.1002/2015GL063655

Ras, J., H. Claustre, and A. C. Uitz. 2008. Spatial variability of phytoplankton pigment distributions in the Subtropical South Pacific Ocean: Comparison between in situ and predicted data. Biogeosciences **5**: 353–369. doi:10.5194/bg-5-353-2008

Rippeth, T. P., P. Wiles, M. R. Palmer, J. Sharples, and J. Tweddle. 2009. The diapcynal nutrient flux and shear-induced diapcynal mixing in the seasonally stratified western Irish Sea. Cont. Shelf Res. **29**: 1580–1587. doi:10.1016/j.csr.2009.04.009

Rudels, B., E. P. Jones, U. Schauer, and P. Eriksson. 2004. Atlantic sources of the Arctic Ocean surface and halocline waters. Polar Res. **23**: 181–208. doi:10.3402/polar.v23i2.6278

Sakshaug, E. 2004. Primary and secondary production in the Arctic Sea, p. 57–81. *In* R. Stein and R. W. MacDonald [eds.], The organic carbon cycle in the Arctic Ocean. Springer.

Schulze, L. M., and R. S. Pickart. 2012. Seasonal variation of upwelling in the Alaskan Beaufort Sea: Impact of sea ice cover. J. Geophys. Res. **117**: C06022. doi:10.1029/2012JC007985

Sharples, J., C. M. Moore, and E. R. Abraham. 2001. Internal tide dissipation, mixing, and vertical nitrate flux at the shelf edge of NE New Zealand. J. Geophys. Res. **106**: 14069–14081. doi:10.1029/2000JC000604

Shen, Y., C. G. Fichot, and R. Benner. 2012. Dissolved organic matter composition and bioavailability reflect ecosystem productivity in the Western Arctic Ocean. Biogeosciences **9**: 4993–5005. doi:10.5194/bg-9-4993-2012

Sherr, E. B., B. F. Sherr, and A. J. Hartz. 2009. Microzooplankton grazing impact in the Western Arctic Ocean. Deep-Sea Res. Part II Top. Stud. Oceanogr. **56**: 1264–1273. doi:10.1016/j.dsr2.2008.10.036

Sherr, E. B., B. F. Sherr, and C. Ross. 2013. Microzooplankton grazing impact in the Bering Sea during spring sea ice conditions. Deep-Sea Res. Part II Top. Stud. Oceanogr. **94**: 57–67. doi:10.1016/j.dsr2.2013.03.019

Terrado, R., K. Scarcella, M. Thaler, W. F. Vincent, and C. Lovejoy. 2012. Small phytoplankton in Arctic seas: Vulnerability to climate change. Biodiversity **14**: 2–18. doi:10.1080/14888386.2012.704839

Tolosa, I., S. Fiorini, B. Gasser, J. Martín, and J. C. Miquel. 2013. Carbon sources in suspended particles and surface sediments from the Beaufort Sea revealed by molecular lipid biomarkers and compound-specific isotope analysis. Biogeosciences **10**: 2061–2087. doi:10.5194/bg-10-2061-2013

Tomas, C. R. 1997. Identifying marine phytoplankton. Academic Press.

Tremblay, G., C. Belzile, M. Gosselin, M. Poulin, S. Roy, and J.-É. Tremblay. 2009. Late summer phytoplankton distribution along a 3500 km transect in Canadian Arctic waters: Strong numerical dominance by picoeukaryotes. Aquat. Microb. Ecol. **54**: 55–70. doi:10.3354/ame01257

Tremblay, J.-É., K. Simpson, J. Martin, L. Miller, Y. Gratton, D. Barber, and N. M. Price. 2008. Vertical stability and the annual dynamics of nutrients and chlorophyll fluorescence in the coastal, southeast Beaufort Sea. J. Geophys. Res. **113**: C07S90. doi:10.1029/2007jc004547

Tremblay, J.-É., and others. 2011. Climate forcing multiplies biological productivity in the coastal Arctic Ocean. Geophys. Res. Lett. **38**: L18604. doi:10.1029/2011gl048825

Tremblay, J.-É., P. Raimbault, N. Garcia, B. Lansard, M. Babin, and J. Gagnon. 2014. Impact of river discharge, upwelling and vertical mixing on the nutrient loading and productivity of the Canadian Beaufort Shelf. Biogeosciences **11**: 4853–4868. doi:10.5194/bg-11-4853-2014

Tremblay, J.-É., L. G. Anderson, P. Matrai, P. Coupel, S. Bélanger, C. Michel, and M. Reigstad. 2015. Global and regional drivers of nutrient supply, primary production and CO_2 drawdown in the changing Arctic Ocean. Prog. Oceanogr. **139**: 171–196. doi:10.1016/j.pocean.2015.08.009

Varela, D. E., D. W. Crawford, I. A. Wrohan, S. N. Wyatt, and E. C. Carmack. 2013. Pelagic primary productivity and upper ocean nutrient dynamics across Subarctic and

Arctic Seas. J. Geophys. Res. **118**: 21. doi:10.1002/2013JC009211

Walkusz, W., W. J. Williams, L. A. Harwood, S. E. Moore, B. E. Stewart, and S. Kwasniewski. 2012. Composition, biomass and energetic content of biota in the vicinity of feeding bowhead whales (*Balaena mysticetus*) in the Cape Bathurst upwelling region (south eastern Beaufort Sea). Deep-Sea Res. Part I Oceanogr. Res. Pap. **69**: 25–35. doi:10.1016/j.dsr.2012.05.016

Watanabe, E., and others. 2014. Enhanced role of eddies in the Arctic marine biological pump. Nat. Commun. **5**: 3950. doi:10.1038/ncomms4950

Wheater, C. P., and P. A. Cook. 2005. Using statistics to understand the environment. The Taylor & Francis e-Library.

Williams, W. J., and E. C. Carmack. 2015. The 'interior' shelves of the Arctic Ocean: Physical oceanographic setting, climatology and effects of sea-ice retreat on cross-shelf exchange. Prog. Oceanogr. **139**: 21–41. doi:10.1016/j.pocean.2015.07.008

Xie, H., S. Bélanger, G. Song, R. Benner, A. Taalba, M. Blais, J.-É. Tremblay, and M. Babin. 2012. Photoproduction of ammonium in the southeastern Beaufort Sea and its biogeochemical implications. Biogeosciences **9**: 3047–3061. doi:10.5194/bg-9-3047-2012

Zar, J. 1999. Biostatistical analysis, 4th ed. Prentice Hall.

Acknowledgments

We are especially indebted to Yves Gratton and Pascal Guillot for providing the physical data, Hervé Claustre for HPLC data, Sylvie Lessard for phytoplankton and other protist identification, and Bernard Gentili for programing advises. We also thank particularly Maxime Benoît-Gagné, Eric Rehm, Thomas Lacour, Pierre Coupel, Anabelle Baya, and the whole Takuvik team for constructive comments on the manuscript. This manuscript was also greatly improved by the detailed and insightful comments of two anonymous reviewers. This is a contribution to the research programs of the CERC in Remote Sensing of Canada's New Arctic Frontier, Takuvik Joint International Laboratory, ArcticNet, Institut des sciences de la mer de Rimouski and Québec-Océan. This project was supported by grants from the Canada Excellence Research Chair (CERC) in Remote Sensing of Canada's New Arctic Frontier, the Takuvik Joint International Laboratory (CNRS and Université Laval), the Network of Centres of Excellence of Canada ArcticNet, the Natural Sciences and Engineering Research Council of Canada and Québec-Océan funded by the Fonds de recherche du Québec–Nature et technologies. M. A. received a postgraduate scholarship from the CERC Remote Sensing of Canada's New Arctic Frontier and stipends from ArcticNet and Québec-Océan.

Conflict of Interest

None declared.

Submitted 26 May 2016
Revised 02 November 2016; 06 February 2017
Accepted 22 February 2017

Associate editor: Heidi Sosik